frontiers | Frontiers in Earth Science

TYPE Review
PUBLISHED 12 April 2023
DOI 10.3389/feart.2023.1143380

OPEN ACCESS

EDITED BY
Amit Kumar Mishra,
Jawaharlal Nehru University, India

REVIEWED BY
Anning Huang,
Nanjing University, China
Krishan Kumar,
Jawaharlal Nehru University, India

*CORRESPONDENCE
Deliang Chen,
deliang@gvc.se

†These authors have contributed equally to this work and share the first authorship

SPECIALTY SECTION
This article was submitted to Atmospheric Science, a section of the journal Frontiers in Earth Science

RECEIVED 12 January 2023
ACCEPTED 27 March 2023
PUBLISHED 12 April 2023

CITATION
Kukulies J, Lai H-W, Curio J, Feng Z, Lin C, Li P, Ou T, Sugimoto S and Chen D (2023), Mesoscale convective systems in the third pole region: Characteristics, mechanisms and impact on precipitation.
Front. Earth Sci. 11:1143380.
doi: 10.3389/feart.2023.1143380

Mesoscale convective systems in the third pole region: Characteristics, mechanisms and impact on precipitation

Julia Kukulies[1†], Hui-Wen Lai[1†], Julia Curio[1], Zhe Feng[2], Changgui Lin[1], Puxi Li[3], Tinghai Ou[1], Shiori Sugimoto[4] and Deliang Chen[1*]

[1]Department of Earth Science, Regional Climate Group, University of Gothenburg, Gothenburg, Sweden, [2]Division of Atmospheric Sciences and Global Change, Pacific Northwest National Laboratory, Richland, WA, United States, [3]State Key Laboratory of Severe Weather, Chinese Academy of Meteorological Sciences, China Meteorological Administration, Beijing, China, [4]Japan Agency for Marine-Earth Science and Technology, Yokohama, Japan

The climate system of the Third Pole region, including the (TP) and its surroundings, is highly sensitive to global warming. Mesoscale convective systems (MCSs) are understood to be a vital component of this climate system. Driven by the monsoon circulation, surface heating, and large-scale and local moisture supply, they frequently occur during summer and mostly over the central and eastern TP as well as in the downstream regions. Further, MCSs have been highlighted as important contributors to total precipitation as they are efficient rain producers affecting water availability (seasonal precipitation) and potential flood risk (extreme precipitation) in the densely populated downstream regions. The availability of multi-decadal satellite observations and high-resolution climate model datasets has made it possible to study the role of MCSs in the under-observed TP water balance. However, the usage of different methods for MCS identification and the different focuses on specific subregions currently hamper a systematic and consistent assessment of the role played by MCSs and their impact on precipitation over the TP headwaters and its downstream regions. Here, we review observational and model studies of MCSs in the TP region within a common framework to elucidate their main characteristics, underlying mechanisms, and impact on seasonal and extreme precipitation. We also identify major knowledge gaps and provide suggestions on how these can be addressed using recently published high-resolution model datasets. Three important identified knowledge gaps are 1) the feedback of MCSs to other components of the TP climate system, 2) the impact of the changing climate on future MCS characteristics, and 3) the basin-scale assessment of flood and drought risks associated with changes in MCS frequency and intensity. A particularly promising tool to address these knowledge gaps are convection-permitting climate simulations. Therefore, the systematic evaluation of existing historical convection-permitting climate simulations over the TP is an urgent requirement for reliable future climate change assessments.

KEYWORDS

Tibetan plateau, mesoscale convective system, precipitation, tracking, satellite observations, convection-permitting climate simulations, Asian monsoons

1 Introduction

The Tibetan Plateau and its adjacent mountain ranges - including the Hindu Kush, Karakoram, and Himalayas - are often nicknamed the Third Pole (TP), because these mountain systems altogether provide the third largest freshwater storage on Earth after the Arctic and Antarctica. There are other parallels that can be drawn between the TP and the first two poles, e.g., the amplified warming (You et al., 2021) and the rapidly decreasing cryosphere (Yang M. et al., 2019), which has turned the region into a highly sensitive ecosystem and a hotspot for climate change (Ehlers et al., 2022; Yao et al., 2022). However, one water cycle component that clearly distinguishes the regional climate of the TP from the other polar climates is atmospheric convection and associated precipitation. The TP is characterized by intense summer convection (Flohn and Reiter, 1968; Qie et al., 2014) and its downstream regions are global hotspots for organized convection over land (Laing and Michael Fritsch, 1997; Feng et al., 2021a) owing to the interplay of midlatitude atmospheric dynamics, moisture supply from the tropics and the influence of mountainous weather systems from the TP (Tao and Ding, 1981; Xu and Zipser, 2011; Curio et al., 2019).

Mesoscale convective systems (MCSs) are complexes or clusters of convective storms that grow upscale into large precipitating systems. MCSs have been found to frequently occur and affect the precipitation in the TP region. Precipitation that is produced by MCSs has crucial hydrological and socioeconomic implications because it can trigger natural hazards such as landslides and flash floods (Schumacher and Rasmussen, 2020) which pose a threat to infrastructure, homes, and lives. Extreme events like rainstorms and devastating floods have been attributed to MCSs that aggregated from diurnally driven convective systems over the TP, at the central TP (Wang S. et al., 2021), the southern foothills of the TP (Rasmussen and Houze, 2012), in the Sichuan basin (Xia et al., 2021), in the Yangtze river basin (Yu, 2001; Yasunari and Miwa, 2006; Xu et al., 2008; Li et al., 2019) and farther away in Eastern China (Tao and Ding, 1981). For example, a flash flood case in the Himalayas was attributed to an MCS producing more than 200 mm of rain within 3 h in a valley that usually has a desert-like climate (Rasmussen and Houze, 2012). In one of the flood-producing MCS cases in the Sichuan basin, gauge stations recorded that about a quarter of the annual rainfall fell within only 24 h (Feng et al., 2014). At the same time, MCSs may affect the seasonal water availability in regions where they contribute substantially to the total rainfall amount on sub-seasonal and seasonal scales (e.g., Kukulies et al., 2021). In the river basins surrounding the TP, summer precipitation is of particular importance because it has been found to play a central role in runoff (e.g., Zhang et al., 2013).

MCSs are a type of organized convection with cloud shields that can vary by more than one order of magnitude in size, but have minimum horizontal extents of ~100 km in the precipitation area (Houze Jr, 2004). The organization of convection into storms involves many different physical mechanisms and the concept of *convective organization* mainly helps to distinguish long-lived clusters of convective clouds from isolated convection. While isolated or *unorganized convection* refers to short-lived convective clouds that occur randomly in time and space, *organized convection* generates an internal circulation that results in the aggregation of several convective cells. Consequently, organized convection is characterized by larger vertical and horizontal extents as well as a longer duration compared to unorganized convection. Although the term MCS is an umbrella that includes different storm types (i.e., squall lines, mesoscale convective complex, *etc.*,; Maddox, 1980), they are clearly distinct from single isolated storm cells. The interaction of multiple storms within an MCS generates mesoscale circulations that help the system persist from several hours (typically > 3 h in the midlatitudes; Houze, 2004) to a day or longer. Globally, MCSs are understood as efficient rain producers due to the relatively long persistence of heavy precipitation and extensive areas of stratiform precipitation associated with them (Houze Jr, 2004).

From a broader perspective, it has been suggested that the anticipated increase in extreme precipitation with global warming is related to an intensification of organized convection in the tropics (Rossow et al., 2013; Roca and Fiolleau, 2020), midlatitudes (Pendergrass et al., 2016; Pendergrass, 2020) and North America (Prein et al., 2017; Haberlie and Ashley, 2019). While there is a consensus that general conditions for storm formation such as atmospheric moisture and instability will globally increase (Schumacher and Rasmussen, 2020), there are many unknowns with regard to the regional impact of such changes. The understanding of climate change impacts on MCSs over the TP and adjacent region is still a relatively new research field. In the TP region, the regional climate and atmospheric moisture supply are to a large extent controlled by large-scale atmospheric systems like the South Asian High (Liu et al., 2013; Lai et al., 2021), the Indian and East Asian summer monsoons (Feng and Zhou, 2012; Lai et al., 2021) and the westerly jetstream (Schiemann et al., 2009; Curio and Scherer, 2016). Since MCSs are sufficiently large to interact with these synoptic systems, it is reasonable to assume that future changes in moisture transport and large-scale wind circulation will have a direct effect on MCS genesis and maintenance. Establishing a solid understanding of MCS characteristics and dynamics in the present climate is, however, a necessary prerequisite for the assessment of region-specific MCS responses to climate change.

The understanding of the multiple scales and processes of mesoscale convective precipitation in the TP region has long been hampered by three main challenges: 1) the low density and heterogeneous nature of ground-based observation networks, 2) high uncertainties in precipitation retrievals from spaceborne measurements over complex terrain, and 3) insufficient spatial resolution of global climate models. We are, however, entering an era wherein improved satellite retrievals and numerical model simulations that can resolve micro- and meso-scale processes are becoming available on multi-decadal time scales. Such novel techniques and datasets represent new opportunities to advance our understanding of MCS characteristics and dynamics in a climate change context, especially in remote regions like the TP, where ground-based observations are still limited.

The potential of new model and observational datasets has resulted in increasing attention on global MCSs during the past decade (e.g., Yuan and Houze, 2010; Prein et al., 2020; Feng et al., 2021a; Schumacher and Rasmussen, 2020). A number of regional climate studies that focus on MCSs in the TP region have also emerged (e.g., Sugimoto and Ueno, 2012; Li et al., 2020; Kukulies et al., 2021). Non-etheless, there are still many open questions with regard to the role of MCSs in the TP water cycle and a big picture is still missing despite the existence of a

mosaic of individual studies that have a narrow focus on specific MCS cases, processes, or subregions. In addition, the existing climatological studies have used many different definitions and methods for MCS identification, which has partly led to ambiguous conclusions about their impact on regional precipitation. Overall, there are two types of MCS studies: 1) those include or focus on MCSs in the humid downstream regions (e.g., Zheng et al., 2008; Li et al., 2020; Kukulies et al., 2021) and 2) those exclusively focus on MCSs over the arid high altitudes of the TP (e.g., Yaodong et al., 2008; Sugimoto and Ueno, 2010; Hu et al., 2016; Liu Y. et al., 2021; Mai et al., 2021; Zhang et al., 2021). While it is certainly useful to distinguish between different MCS types in a highly diversified region like the TP and its surroundings, there is also a need to disentangle the relative importance of these MCS types and to revisit the role of convection over the TP for precipitation and MCS formation in the downstream regions. The current literature prompts several unanswered questions: *How often do MCSs actually occur over the TP, given that the moisture supply is rather limited at higher altitudes? How important are MCSs over high altitudes in terms of total precipitation that potentially controls river runoff compared to MCSs in the downstream regions? Do MCSs or smaller isolated convection over the TP influence downstream MCS formation?*

A holistic synthesis in which the TP and its downstream regions are regarded as a coupled system might clarify some of these questions and help to identify key processes that need to be addressed in future studies. In this review, we aim to provide such a synthesis with the ultimate goal to present the current understanding and critical knowledge gaps that are relevant for the TP community as well as for the wider research field. More specifically, we aim to synthesize what we know about present-climate characteristics, mechanisms, and precipitation impact of MCSs in the TP region by linking their key statistics (what do we observe?) to their dynamics and physical theory (what processes cause the observed features?).

The remainder of this paper is structured as follows: In **section 2**, we review spatiotemporal characteristics of MCSs revealed by satellite-based observations and their impact on regional precipitation. In **Section 3**, we link these observed characteristics with physical processes at different spatial scales and identify key mechanisms that have been suggested for MCS genesis and maintenance. Here, we also consider mechanisms that have been found relevant in other major mountain regions and discuss their potential relevance in the TP region. In **Section 4**, we summarize general challenges and new opportunities in observing, modeling, and identifying MCSs in the TP region. Finally, we present the identified knowledge gaps and suggestions for how these can be addressed in future research in **Section 5**.

2 Satellite-derived key characteristics

2.1 Identification of MCSs

One can easily observe MCSs from space because they produce extensive stratiform cloud shields and deep convective clouds that appear particularly cold in infrared (IR) and particularly bright in visible satellite imagery owing to the low cloud-top temperatures and high reflectance, respectively. The most common method to collect information about MCSs over time is thus to identify large, cold cloud objects in satellite observations using an automated tracking algorithm. For this, different meteorological fields that are relevant for convection can be used, e.g., IR brightness temperatures (Tb; as a proxy for cloud-top temperatures), radar reflectivity, or surface precipitation (Feng et al., 2019; 2021a; Haberlie and Ashley, 2019). Compared to case studies, such object-based analyses have the advantage of capturing statistics about MCS frequency, intensity, and duration over longer time periods, which helps to better understand the role of MCSs in the water cycle and in the climate context. However, the challenge with using automated tracking methods to identify MCSs is finding a robust set of criteria and thresholds that are applicable for regions with different background climates. For example, the TP region includes large areas with elevations above 4,000 m a.s.l, whereas its surrounding areas are close to sea level. The criteria that work well to identify MCSs in the surrounding regions might therefore lead to biases in MCS detection over the TP. In particular, the background brightness temperatures are generally colder over the TP compared to lower elevation areas at the same latitudes. Because many MCS tracking methods identify cold features in IR satellite imagery, there may have been an overemphasis on MCSs over the TP.

Feng et al. (2021a) and Kukulies et al. (2021) showed that the total number of identified MCSs over the TP reduces substantially when intensity and area thresholds are applied to surface precipitation and brightness temperatures instead of brightness temperatures only. The reason for this is that high cirrus clouds or synoptically-driven cloud systems over high mountain regions can produce cold cloud features similar to deep convective clouds in warm climate regions, as was also noted by Esmaili et al. (2016). Combining brightness temperatures with precipitation estimates provides additional constraints to the identified cold cloud clusters that are associated with larger areas of heavy precipitation. This type of multivariable tracking method helps eliminate cold cloud systems that do not produce significant precipitation and improves the detection of MCSs in the mid-latitudes where many large cold cloud systems are not associated with MCSs. Moreover, using precipitation as a proxy for MCSs is useful for application-based studies due to its relevance for flooding. It can also be easier to directly compare precipitation with climate model output, even though outgoing longwave radiation, which is a standard output variable, can be converted to brightness temperatures (e.g., Feng et al., 2021b). Despite the advantages of using precipitation as an MCS proxy, most studies in the TP region have detected MCSs based on IR satellite imagery only, because high-resolution satellite retrievals of sub-daily precipitation have only recently become available for multiple decades (e.g., Joyce et al., 2004; Huffman et al., 2019).

Figure 1 shows two example snapshots of brightness temperatures from geostationary satellites (NCEP/CPC) overlayed with precipitation estimates from GPM IMERG (as in Feng et al., 2021a; Kukulies et al., 2021; Zhang et al., 2021). The brightness temperature data makes it possible to capture the full lifecycle and spatial coverage of an MCS (not only its raining part), while the precipitation data reveals which part of the detected cloud is associated with surface precipitation. There are multiple MCSs in **Figure 1A** including a relatively large and almost circular MCS close to the eastern edge of the TP (~ 105°E). **Figure 1B** shows an MCS detected within the 3000-m elevation boundary of the TP. While its

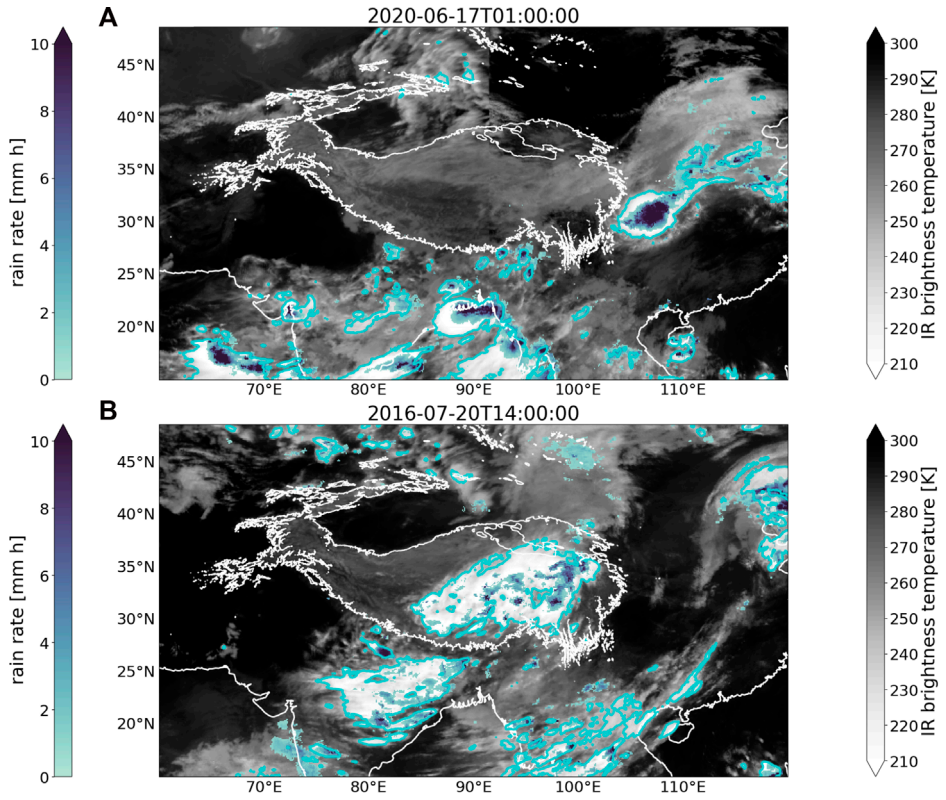

FIGURE 1
Two example snapshots of hourly IR brightness temperatures overlaid with hourly precipitation estimates from GPM IMERG. The turquoise lines indicate the 241 K contour, a commonly used threshold to define the cloud area of an MCS. **(A)** shows an MCS that occurred at the downwind side of the TP in June 2020. **(B)** shows an MCS that formed over the TP. The white contour line over land is the 3000 m elevation contour of the TP.

cloud shield extends over a large area, the regions with heavy surface precipitation are not organized into a larger contiguous area as in typical, unambiguous MCS cases (e.g., Houze, 2004). The scattered precipitation suggests that the convective features of this system might be embedded in the synoptic circulation rather than having its own mesoscale circulation. This exemplifies how characteristics of convection over the TP might differ from MCSs in the lower elevated downstream regions, even though both cases fulfill the same minimum criteria to be classified as an MCS according to the tracking algorithm in (Kukulies et al., 2021,; **Table 1**).

Using different meteorological fields to track MCSs is not the only source of uncertainty in deriving climatological MCS features. Currently, there is no common standard used for MCS tracking, and the applied detection criteria on intensity, time persistence, and spatial extent differ substantially in the literature. This is not only true for the TP region, and makes it in general difficult to interpret and compare the results from different MCS studies. **Table 1** summarizes the different criteria that have been used to identify MCSs in the TP region based on satellite observations. For studies that include the high mountains of the TP, the most common set of thresholds is that the cloud shield (defined by IR Tb <221 K) of an MCS must cover an area <5,000 km^2 for at least consecutive 3 h (**Table 1**). However, the IR temperature and area thresholds exhibit large variations even among studies that cover almost the same regions. In the next section, we show how this has led to seemingly inconsistent conclusions about the importance of MCSs in different regions and their impact on precipitation.

2.2 Spatial and temporal distribution and scales

Figure 2 compares two estimations of MCS frequencies for the wider TP region derived from the MCS climatologies created by Kukulies et al. (2021) and Feng et al. (2021a). While both climatologies are based on the same data (brightness temperatures from geostationary satellites co-located with gridded satellite retrievals of surface precipitation), they have been constructed using different criteria and tracking algorithms for MCS detection (**Table 1**). The general spatial pattern is consistent and shows the Indo-Gangetic Plains and the lower Mekong river basin as regions with the largest numbers of MCSs over land. Another common feature is the mid-latitudinal gradient of MCS frequencies over China and the connected area between the eastern edge of the TP and its eastern downstream region. In general, Feng et al. (2021a) shows slightly higher counts of individual MCS tracks over some land areas like Eastern China, whereas Kukulies et al. (2021) shows higher MCS frequencies over the Bay of Bengal (**Figure 2**). Since these discrepancies can only stem from the applied thresholds and tracking method, they may reflect the difference in the required

TABLE 1 Criteria used for MCS identification based satellite observations over the Third Pole region (modified and updated from Kukulies et al. (2021)).

Region	Time period	Tb threshold [K]	Threshold for rain rate [mm hr^{-1}]	Additional criteria?	Minimum extent [km^2]	Minimum duration [hrs]	Reference per year or season	Nr. Of identified tracks
80 °E–105 °E, 27 °N–40 °N	1998	241	–	–	1,000	3	Guo et al. (2006)	749/Jun-Aug
75 °E–105 °E, 25 °N–40 °N	1998–2001	245	–	221 K overshoot Tb	27,000	–	Yaodong et al. (2008)	160 (Jun-Aug)
80–145 °E, 10 °N-55 °N	1996–2006	221	–	–	50,000	–	Zheng et al. (2008)	–
70 °E–103 °E, 29 °N–40 °N > 3500 m	1998–2006	219	–		4,000	6	Sugimoto and Ueno. (2010)	290/year
70 °E–130 °E, 10 °N–60 °N	1996–2008	227	–	–	5,000	3	Jun et al. (2012)	6949/year
70 °E–140 °E, 18 °N–55 °N	2005–2012	221	–	Eccentricity and geometric shape	30,000	3	Yang et al. (2015)	1,087/year
75 °E–105 °E, 25 °N–40 °N > 3,000 m	1998–2004	245	–	optical depth ≤23	25,000	3	Hu et al. (2016), Hu et al. (2017)	106
106 °E–113 °E, 28 °N–35 °N	2000–2016 excluding 2005	221	–		5,000	3	Yang et al. (2019b)	20/May-Aug
80 °E–150 °E, 0 °N–55 °N	2016	235	–	max area of 160,000 km^2	10,000	3	Chen et al. (2019)	41,334/Apr-Sep
102.58 °E–121.58 °E, 21.08 °N–38.08 °N	2008–2016	–	3		3,600	6	Li et al. (2020)	420
105 °E-123 °E, 28 °N-35 °N 105 °E-123 °E, 20 °N-27 °N	2014–2018	241	–	225 K overshoot Tb	60,000	6	Cui et al. (2020b)	30/May-Sep
75 °E–103 °E,26°N-40°N > 3,000 m	2000–2016	221	–	–	5,000	3	Mai et al. (2021)	609/May-Sep
75 °E–103 °E,26°N-40°N	2013–2019	240	max precip >2 mm h^{-1}, precipitating area >200 km^2	225 K overshoot Tb	5,000	–	Zhang et al. (2021)	1,260/yea

(Continued on the following page)

10.3389/feart.2023.1143380

TABLE 1 (*Continued*) **Criteria used for MCS identification based satellite observations over the Third Pole region (modified and updated from Kukulies et al. (2021)).**

Region	Time period	Tb threshold [K]	Threshold for rain rate [mm hr^{-1}]	Additional criteria?	Minimum extent [km^2]	Minimum duration [hrs]	Reference per year or season	Nr. Of identified tracks
100 °E–130 °E, 18 °N–35 °N	2008–2017	–	5	–	3,600	10	Yun et al. (2021)	243/year
100 °E–114 °E, 24 °N–35 °N	2009–2018	221	–	–	5,000	3	Meng et al. (2021)	302/year
65 °E–120 °E, 15 °N–50 °N°N	2000–2019	221	>10% of cloud area must be >5 mm h^{-1}	200 K overshoot	10,000	3	Kukulies et al. (2021)	1,267/year (1,207/Jun-Aug)
Global, subregion over East Asia: 65 °E–120 °E, 15 °N–50 °N	2000–2021	241	100 km precipitation >2 mm h^{-1} Life-time dependent thresholds for precipitation	225 K overshoot Tb	40,000	4	Feng et al. (2021a)	1,616/year (967/Jun-Aug)
82 °E-103 °E, 27 °N-40 °N	2005–2012	221	–	Eccentricity and geometric shape	30,000	3	Liu et al. (2021b)	183/May-Aug
100 °E-108 °E, 28 °N-38 °N	2000–2018	221	–	–	5,000	3	Guo et al. (2022)	102/May-Aug

10.3389/feart.2023.1143380

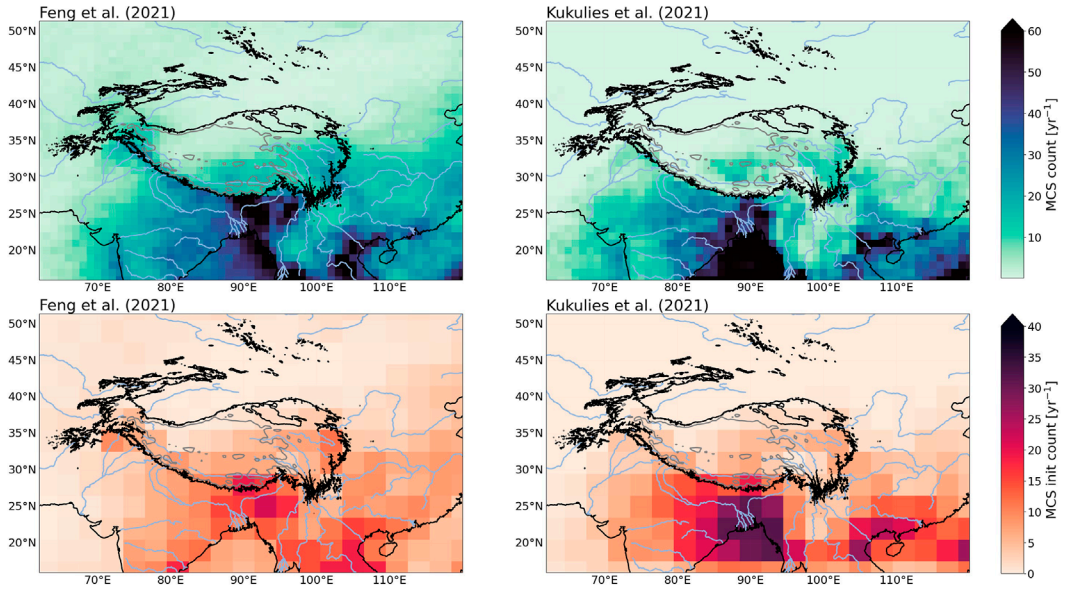

FIGURE 2
Spatial distribution of average MCS frequency throughout all lifecycle stages (upper panels) and MCS initiation frequency (lower panel) per year based on the datasets constructed by Kukulies et al. (2021); Feng et al. (2021a). The total number of MCSs has been computed based on their center locations on a 1x1° grid for every time step and for 1x1° on a 3x3° grid for the time steps of detection (initiation). The two MCS climatologies have been constructed independently, but based on the same infrared brightness temperatures from geostationary satellites combined with GPM IMERG v06 precipitation estimates. The black and gray contours show the 3000 m and 5,000 m elevation boundaries, respectively.

minimum cloud area (e.g., leading to more coherent and longer tracks for lower thresholds and hence more frequent MCSs) as well as the different treatment of merging and splitting (that affects the total number of MCSs when individual tracks break off).

Figure 3 demonstrates that the total number of MCSs per year exhibits generally large variations across the same regions due to different tracking criteria (**Table 1**). Here, we compare the average annual MCS frequencies normalized by the area of the region in which the tracking was performed. The hatched bars denote studies that have only focused on the TP and the black edges denote studies that have included precipitation as verification in their tracking method. The gray bars show the MCS counts obtained from the global MCS tracking from Feng et al. (2021a) matched to the same domain, time periods, and season to each of the regional studies. Although the frequencies are normalized by the area of the different study regions, there are considerable differences in total MCS numbers between the studies. While it is expected that larger regions that cover parts of the tropical ocean (e.g., Jun et al., 2012; Chen et al., 2019), differ from smaller regions that have a more homogenous climate (e.g., Sugimoto and Ueno, 2010; Liu Y. et al., 2021), it is discernible that TP studies show significantly different numbers, even though their domains are similar (e.g., Hu et al., 2016; Zhang et al., 2021) or identical (e.g., Feng et al. (2021a) compared to Chen et al. (2019)). These discrepancies can be partly explained by the fact that some studies only include the warm season while others include the entire year (**Table 1**). Although it is expected that most MCSs occurs during the warm season near the TP and the lower plains, studies covering large parts of the tropics would detect substantially higher numbers of MCSs because MCSs occur also during the boreal winter season in these regions (see Figure 11 in Feng et al., 2021a). However, the comparison with Feng et al. (2021a) shows that the MCS number is not a robust metric for the comparison of MCS statistics obtained by different tracking algorithms because many factors influence how an MCS track is defined. The large difference between Feng et al. (2021a) and Chen et al. (2019) may, for example, result from the fact that Chen et al. (2019) apply considerably lower thresholds and use satellite data with a higher spatial resolution (hence allowing for more clouds to be tracked) compared to Feng et al. (2021a). The treatment of merging and splitting as well as the method to combine cloud objects from different time steps are other factors that might substantially affect the resulting number of tracks.

Furthermore, there is a large spread among different downstream regions on the lee side of the TP (Cui et al., 2020b; Li et al., 2020; Meng et al., 2021) which are most likely explained by the different tracking methods but could also partly reflect the regional and temporal differences in MCS occurrences over China. As pointed out by Zheng et al. (2008), MCSs over land exhibit the largest inter-annual fluctuations around the latitude band of ~ 30°N. We note that this could be due to midlatitude eddies controlling moisture supply and atmospheric instability in contrast to the tropical monsoon regions, where moisture and energy supply are almost always abundant. However, the current literature reveals only little about the impact of inter-annual to sub-seasonal variations in moisture transport on MCS distributions in the downstream regions of the TP.

Since MCSs are closely linked to the propagation of the Asian summer monsoon, they occur mainly between June and August. Even though MCSs east of the TP are also present during the springtime (Li et al., 2020), the summer peak of MCS occurrences

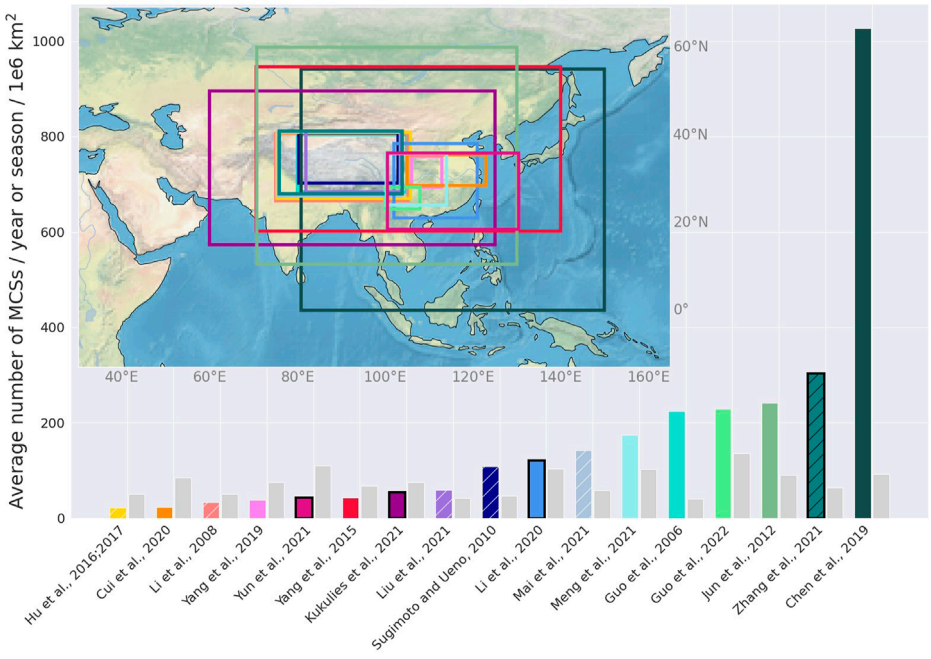

FIGURE 3
Overview of average MCS frequencies as found by different regional studies. The color-coded domains in the map correspond to the extent that was used for MCS tracking in the studies with the same color in the bar plot. Hatched bars mark studies that have focused on the TP in contrast to studies that have included or focused on the downstream regions. The bars with black edges denote the studies that have included precipitation as a criterion in their tracking, in contrast to studies that have used brightness temperatures only. The gray bars are from the global MCS tracking dataset from Feng et al. (2021b) matched to the same domain, time periods, and season to each of the regional studies. Note that, for a fair comparison, annual MCS frequencies have been normalized by the area of the tracking domain, so the average number of detected MCSs refers to the same area size.

is consistent between all studies and sub-regions around the TP. The diurnal cycles of MCS genesis and maturity show, in contrast, much larger regional differences because these are controlled by local and regional weather regimes such as mountain-valley breezes or land-ocean contrasts of surface heating (e.g., Kukulies et al., 2021). The duration of MCSs over the TP is generally shorter compared to MCSs in the downstream regions, suggesting that convection over the TP is less organized (Feng et al., 2021a; Kukulies et al., 2021). This difference in lifetime is also linked to regional variations in the diurnal cycle, because the shorter-lived systems over the moisture-limited TP result in a single-peak of MCS genesis, whereas longer-lived MCSs in the plains are marked by multi-peak diurnal cycles. Where moisture is abundant, MCSs may decay in the evening and re-intensify during nighttime (Zheng et al., 2008). MCSs over mainland China are relatively long-lived with an average lifetime of more than 6 h, even during spring and autumn (Li et al., 2020). A region that is marked by particularly long-lived systems is the Sichuan basin, where a quarter of detected MCSs prevail longer than 18 h (Li et al., 2020,; see **Table 1** for criteria).

Although there is evidence that a large part of the plateau-scale precipitation over the TP occurs as convective precipitation (Maussion et al., 2014; Kukulies et al., 2019), the spatial scales of summer convection have not yet been systematically quantified. Observational studies based on space-borne radar measurements have shown that convective precipitation over the TP occurs in isolated rather than in organized form (Houze Jr et al., 2007; Romatschke and Houze, 2011; Houze Jr et al., 2015). For example, 3D echoes from the Tropical Rainfall Measurement Mission show that there are deep convective cores but no wide convective cores over the TP during summer, where the latter are defined as intense convection over areas ~ 1,000 km^2 (see Figure 6 in Houze Jr et al. (2015)). In addition, Kukulies et al. (2021) showed that MCSs detected over the TP are substantially smaller in size than MCSs in the east and south of the TP. It seems reasonable that the limited moisture supply over the high mountains hampers the degree of convective organization, and we notice that studies that emphasize the high numbers of MCS occurrences over the TP mostly rely on brightness temperatures only. Since the importance of MCSs for the water cycle and for societal impact is mainly materialized through the impact on precipitation, we will review how the spatial characteristics of MCS activity are linked to seasonal and extreme precipitation in the TP region.

2.3 Impact on mountain and downstream precipitation

The impact of MCSs on regional precipitation in the TP region is three-fold: 1) In some regions, MCSs contribute significantly to the total annual precipitation. Even if the absolute amount of total annual precipitation is small, this means that they represent an important component in the regional water cycle with the potential to control other components such as soil moisture and river runoff. 2) In regions that show high MCS contributions to total annual

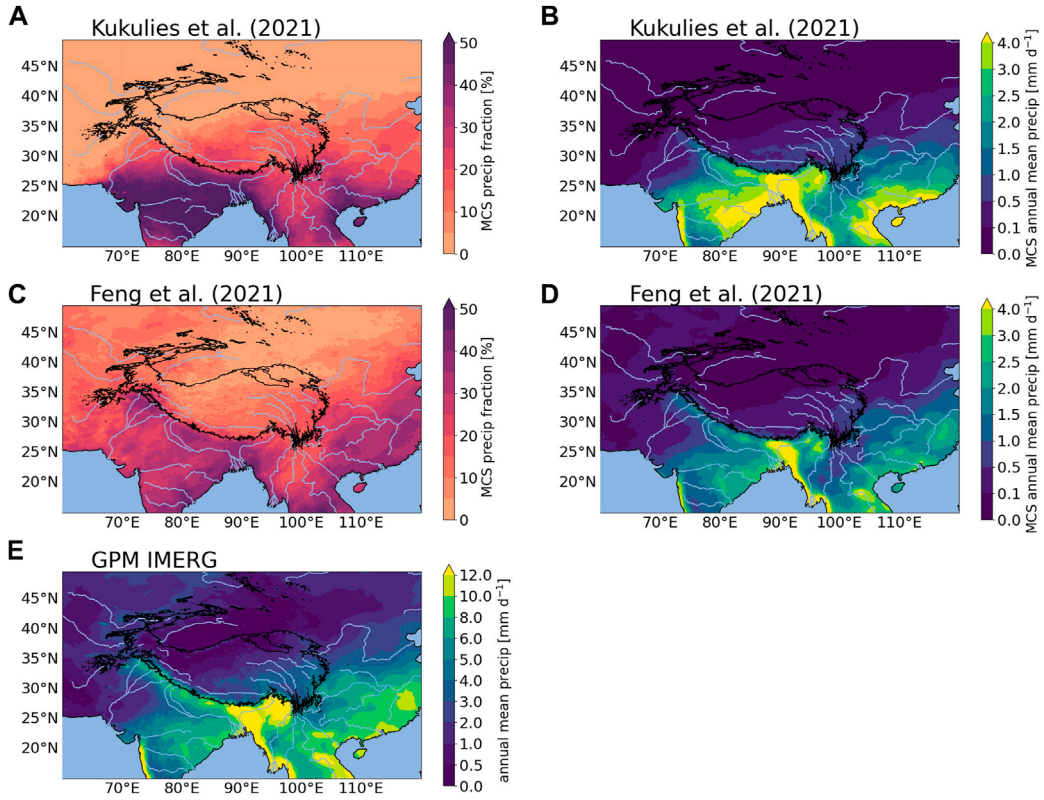

FIGURE 4
Impact of MCSs on precipitation over the TP and its downstream regions over land. Their impact is shown in terms of relative contributions to total annual precipitation [%] **(A,C)** and absolute annual mean precipitation produced by MCSs [mm] **(B, D)**, as calculated in Kukulies et al. (2021); Feng et al. (2021b) based on IR brightness temperatures and satellite precipitation estimates. The MCS-associated precipitation is the total sum of precipitation underneath the detected cloud shield. For context, the total annual mean precipitation from GPM IMERG 2000–2019 is also shown in **(E)**.

rainfall and total absolute amounts of annual rainfall, MCSs can be seen as prolific rain producers with the potential to largely affect and alter water availability. 3) In dry regions, MCSs are not frequent, but might still be important for extreme precipitation, as they can produce large amounts of rainfall over short periods of time and trigger natural hazards, in particular in regions that are not constantly exposed to large amounts of rainfall.

Figure 4 compares the first two aspects by showing the regional distribution of MCS precipitation in relative (a,c) and absolute (b,d) terms. The total annual mean precipitation is also shown for comparison (e). There is a clear tropics-to-midlatitude gradient with the largest contributions and the largest total amounts of MCS rainfall south of the Himalayas, over the Indian continent, and in the coastal areas. Over the TP, MCSs are estimated to contribute between 20% and 30% to total annual precipitation. Similar fractions of MCS rainfall can be found in the adjacent eastern downstream regions, but it should be noted that the total amount of MCS precipitation is considerably higher than MCS precipitation over the TP (**Figure 4E**).

Similar to MCS frequency, different studies have estimated significantly different contributions of MCSs to total precipitation over the TP and in the surrounding regions (**Table 2**). For example, Hu et al. (2016) found that about 70% of the total precipitation over the TP can be attributed to MCSs, whereas Kukulies et al. (2021) and Feng et al. (2021a) showed significantly lower contributions. While these estimations are affected by the different tracking criteria and by the method how precipitation is attributed to an MCS, the contribution to precipitation is a metric that should not be affected by how different tracking algorithms count individual MCSs. This is because the contribution of MCSs to total precipitation in a certain region is mainly affected by how often MCSs occur and how large and intense the detected systems are. It is, however, less important if the MCSs are classified as one unique system or if they are counted as multiple different systems. The total number of individual MCS counts is highly dependent on how different tracking formulations link the features between time steps and how they handle merging and splitting. This implies that even if different tracking algorithms detect comparable numbers of MCS features in each time step, these features are likely to be divided into different numbers of individual MCS tracks. Metrics that are not affected by the total count of individual MCSs might, therefore, give a more robust estimate of MCS occurrences. The relatively small contributions of MCSs to total precipitation in Chen et al. (2019; **Table 2**) together with their outstandingly high number of individual MCSs (**Figure 3**) show that comparisons between MCS studies depend highly on the metric that is chosen. In other words, tracking methods that detect high numbers of MCSs do not necessarily show higher contributions to total precipitation. Given that the MCS contributions are not largely affected by the linking method or MCS counting, the large discrepancies between studies (e.g., Hu et al. (2016) compared to

TABLE 2 How much of the total precipitation is produced by MCSs in different subregions?

Reference	TP	Eastern TP	Upper Mekong river basin	Sichuan basin	Yangtze river basin	Mainland China	Indian subcontinent	East Asia (incl. Ocean)
Feng et al., 2021a	0–25 %	10–25 %	20–45 %	20–25 %	25–45 %	10–45 %	30–60 %	0–90 %
Kukulies et al. (2021)	0–10 %	5–15 %	10–30 %	15–20 %	20–30 %	5–40 %	40–90 %	0–90 %
Hu et al. (2016)	~70 %		30–40 %	30–70 %				
Li et al. (2009)		>60 %				20–60 %		
Guo et al. (2022)			6–18 %					
Yun et al. (2021)						19 %		
Cui et al. (2020a)								
Yang et al. (2019b)		>35 %						
Mai et al. (2021)	~20 %							
Chen et al. (2019)								6–17 %
Meng et al. (2021)				>30 %				
Li et al. (2021)					>30 %			

10.3389/feart.2023.1143380

TABLE 3 Factors that affect the genesis and development of MCSs around the TP.

Scale	System/Factors	Influence on MCSs
Large-scale	Plateau heating	Surface diabatic heating Flohn. (1957); Yeh (1957); Yanai et al. (1992)
	Monsoons	CAPE modulating Choudhury et al. (2016); Virts and Houze (2016), water vapor advection Kukulies et al. (2021)
	Westerly jet	MCS moving direction Chen et al. (2020b), precipitation distribution
	Surface moisture	Moisture supply Barton et al. (2021)
Synoptic-scale	Trough	Baroclinic instability Zhu and Chen (2003); Ueno et al. (2011)
	Vortex/TPV	Enhance and maintain MCS activities (Fu et al., 2019, Kukulies et al., *revision submitted to Climate Dynamics*)
	Low-level convergence	Updrafts and moisture supply
	Wind shear	Support MCS activity (no studies for TP)
Mesoscale	Diurnal cycle/CAPE	Convective instability (Sugimoto and Ueno, 2010, 2012)
	Orographic effects	Enhance vertical motion and moisture convergence at the windward Houze Jr et al. (2007); Romatschke et al. (2010); Kotal et al. (2014)
Microscale	Rimming and aggregation in clouds	Precipitation intensity Chen et al. (2020b)

Kukulies et al. (2021); **Table 2**) point toward the importance of the chosen thresholds that define the area and occurrence frequency of cloud features classified as MCSs.

3 Factors that influence MCS genesis and characteristics

The total amount of precipitation produced by an MCS and its impact on society depends largely on how frequent, intense and long-lived they are. It is thus essential to identify under what conditions MCS genesis is favored and what factors control their maintenance. This section reviews various factors that influence MCS development in the TP region, ranging from favorable synoptic circulation systems to mesoscale and microscale processes that affect the growth of MCSs. Here, we also review the feedback from MCSs back to the large-scale circulation to discuss their potential impact on the water cycle.

A summary of the main factors and processes for MCS genesis in the TP region is given in **Table 3**.

3.1 Large-scale/synoptic circulation and favorable background conditions for MCS genesis

3.1.1 Advection of water vapor and instability

As noted earlier, a key ingredient for MCS genesis over land is moisture supply which can be either provided by local surface evaporation or by large-scale advection of water vapor from distant oceans and/or land. Because the Asian summer monsoons are associated with low-level jets that transport large amounts of water vapor from the ocean to the continental areas during summer, most of the MCSs over the TP and in the surrounding regions occur in the summer monsoon season. Another key ingredient of convective organization is atmospheric instability in the lower troposphere which can, for instance, be measured by the amount of convective potential available energy (CAPE). The Indian continent is one of the regions in the world, where large amounts of CAPE can accumulate, which upon release produces very intense convection (Zipser et al., 2006). The Asian summer monsoons affect MCS populations around the Himalayan foothills not only by large-scale moisture supply but also by modulating CAPE and wind shear (Choudhury et al., 2016). While MCSs around the Himalayan foothills are associated with the intensity of monsoon circulations and their moist air advection, Virts and Houze (2016) pointed out that MCSs that are closer to mountain regions respond to a larger extent to local CAPE than to large-scale circulation systems. This suggests that markedly different environments are relevant for MCS activities in mountain regions compared to the lower elevated surrounding basins that have less complex topography.

Convective systems over the TP can not only originate from convective instability but also under different wind circulations such as wind shear, vortex, and low-pressure systems (Hu et al., 2016). While the convective systems investigated by Hu et al. (2016) refer to smaller-scale, isolated systems, these might eventually develop into MCSs at later stages. In general, MCSs over the TP might be triggered by low-level convergence under a large-scale condition

when upper tropospheric anticyclone expenses eastward with an intensifying near-surface low pressure in the western plateau (Guofu and Shoujun, 2003; Sugimoto and Ueno, 2010). A synoptic trough accompanied by baroclinic instability could be also favorable for MCS genesis over the TP (Guofu and Shoujun, 2003; Zhu and Chen, 2003). Chen and Li (2021) showed a case of MCS developed at the eastern edge of the TP was under a condition with a western Pacific subtropical high at the east of the precipitation area and a low-pressure system over the TP. Another MCS case was thought to be generated under the convergence between southwesterly monsoon flow and northerly flow associated with a midlatitude trough (Ueno et al., 2011).

3.1.2 Tibetan Plateau vortices

Tibetan Plateau vortices (TPVs) have widely been recognized as weather systems that can affect heavy precipitation events in the downstream areas east of the TP (e.g., in the Sichuan basin; Curio et al., 2019). TPVs are frequently occurring meso-α-scale cyclonic low-pressure systems that are commonly identified as local maxima in relative vorticity close to the surface of the TP (around 500 hPa Feng et al., 2014; Curio et al., 2019). While they originate mainly in the northwestern regions over the TP, they are transported with the prevailing westerly circulation and can, under certain conditions, move off the TP where they influence the weather and potentially trigger precipitation. TPVs can even have far reaching impacts. Sugimoto (2020) identified the eastward propagation of TPVs as a driver of the abundant moisture transport leading to extreme precipitation events over southwestern Japan. While it has been suggested that TPVs can help to enhance or maintain downstream MCS formation (Kukulies et al., *revision submitted to Journal of Climate*), it has not yet been systematically quantified how often TPVs act as a dynamical forcing for MCS formation. Similar sub-synoptic scale disturbances propagating eastward over the Rocky Mountains (Wang et al., 2011) have been linked to the initiation of summer MCSs in the United States under unfavorable large-scale environments (Song et al., 2021). The formation of TPVs might, in turn, also be influenced by the convective organization itself (Fu et al., 2019). The interaction between TPVs and MCSs is therefore an open research topic that needs to be addressed to elucidate the importance of TPVs in moderate and extreme MCS events.

3.1.3 Leeside MCSs

Eastward-moving convective or low-pressure systems can induce cyclogenesis downstream at the eastern edge of the TP and MCS in the downstream area (Yasunari and Miwa, 2006). Hu et al. (2016) showed that convective systems generated over the TP can propagate out of the TP (e.g., 26% moving out eastward and 23% moving out southward), which are essential to the convective precipitation and MCS downstream. Kumar et al. (2014) presented a case of westward propagating MCS together with low-level moist air from the Arabian Sea and Bay of Bengal caused heavy rainfall in a valley near the southwestern TP. Another case showed an eastward propagating cloud system due to prevailing westerly jets forming a downstream rain band with moisture supply from the Western North Pacific subtropical high (Chen Y. et al., 2020).

The diurnal propagation of precipitating systems from the mountains moving eastward is similar to that in the Rocky Mountains (e.g., Carbone et al., 2002; Tucker and Crook, 1999). In the initial phase, maintenance of deep convection and mesoscale systems are locked to afternoon convection over the Rockies. Later, the systems resulted in nocturnal maxima precipitation downstream and moved in the general direction of "steering-level winds" that are essential for not only the locations of the MCSs but also provide a favorable environment for MCS development. The Hovmöller diagrams in **Figure 5** depict the diurnal cycle of eastward propagation of summer precipitation downstream to the TP created from 20 years of half-hourly satellite retrievals from GPM IMERG. Here, we can see that rain rates increase in the eastern TP (~100 °E) during the afternoon. From late evening to early morning the next day, the precipitating systems re-intensify when moving out from the east edge of the TP into the more moist lower-elevated basins (~103 °E). This relationship between mountain convection and downstream precipitation can be seen in all three summer months with June exhibiting the strongest convection over the eastern TP (**Figure 5**).

3.1.4 Feedbacks of MCS to synoptic circulation

While most MCS studies in the TP region focus on the driving mechanism of MCS formation, only few have explored how MCSs feedback to the synoptic circulation. Overall, convective activity over the TP can cause the formation of mesoscale plateau-edge cyclogenesis (Yasunari and Miwa, 2006), which, in turn, triggers so-called southwest vortices. In addition, these systems not only affect features within the troposphere but are also crucial for transporting water vapor to the global stratosphere during summer seasons (Fu et al., 2006; Chen and Li, 2021) show that MCSs can modulate the Asian monsoon cycles, such as onset dates, by providing diabatic sources.

Over the TP, latent heat release by active cloud convections contributes to the variations of the Asian monsoon circulation (Luo and Yanai, 1984; Yanai and Li, 1994). Changes in temperature and specific humidity affect large-scale condensation and circulation (e.g., strength of the Asian monsoons; Li and Zhang, 2017). Large-size MCSs generated over the TP have also been shown to contribute to the eastward extension of the South Asian High (Sugimoto and Ueno, 2012).

The feedback of MCSs in other regions (e.g., the United States) to large-scale circulations has been widely studied. For example, MCSs in the United States have been found to substantially redistribute heat, moisture, and momentum in the lower and middle troposphere (Houze Jr, 2004). In addition, the presence of MCSs can also enhance the environments that are favorable for maintaining MCSs themselves by strengthening the synoptic trough and enhancing the mesoscale vortex behind the MCS (Yang et al., 2017; Feng et al., 2018). Such feedback from MCSs over the TP area has not been well explored and should be addressed in future research.

3.2 Mesoscale and microscale conditions for MCSs

3.2.1 Mountain-valley breeze

The formation and development of convective activities and phase differences in the diurnal cycle over the southern TP are strongly influenced by mountain-valley terrain (Yang et al., 2004;

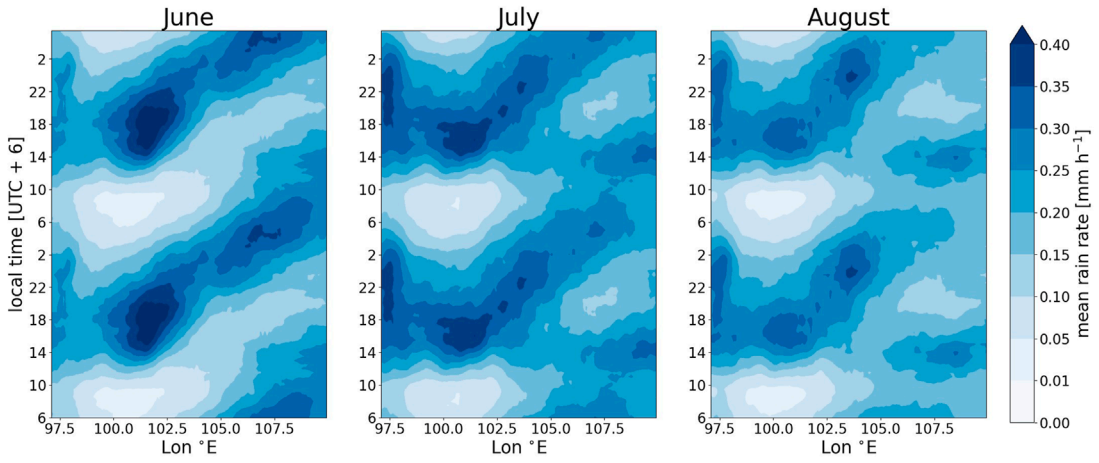

FIGURE 5
Hovmöller (time-longitude) diagrams showing the diurnal propagation of summer precipitation from the eastern edge of the TP (~100 °E) to its downstream regions on the leeward side for June, July, and August. The climatological mean rain rates were computed from half-hourly GPM IMERG v06 data for the time period 2000–2019 and averaged over latitudes 28 °N-34 °N. The diurnal cycle is repeated twice for clarity.

Fujinami et al., 2005), low-level convergence by mountain–valley breezes, and land-sea breezes (Ohsawa et al., 2001; Chen et al., 2005; Fujinami et al., 2005; Hirose and Nakamura, 2005; Yaodong et al., 2008). The dominant factors can be the regional heterogeneous surface heating and the moisture blocking and lifting by the terrain. The convective precipitation peaks often occur from the afternoon to midnight (Kuwagata, 1997). With a more intensive effect from the surface heating and the orographic effect, the convective activities could be enhanced and develop into MCSs. The following will show some examples in detail.

3.2.2 Sensible heating

As thermally-driven circulation is one of the key factors to force vertical motion in convective systems, the relatively stronger solar radiation and consequent diabatic heating at the high elevations of the TP create a favorable environment for MCS development (Fu et al., 2021). The TP is a heating source during summer because surface heating at the high elevation is much higher than surface heating at lower elevations at similar latitudes. Flohn (1957) and Yeh (1957) found a thermal anticyclone in the mid-troposphere above the highlands in Central Asia, slightly located toward the east during summer. This high-pressure system weakens the westerly subtropical jet over North India, reverses the meridional gradient of pressure, and creates a new jet north of Tibet. The summertime sensible heating is not only favorable for convection but the large diurnal change of surface temperature also influences the diurnal cycle of convective activities (Yanai et al., 1992).

The distinct diurnal cycle has not only been observed for precipitation, but also for cloud activity over the TP during the monsoon seasons (Yanai and Li, 1994; Asai et al., 1998)). Large MCSs preferably generated during the daytime by the dominant land surface heating with the low-level convergence under the condition of a prevailing upper tropospheric anticyclone in reanalysis data (Sugimoto and Ueno, 2010; 2012). Previous studies showed that an MCS case over the TP was developed in a thick, convectively unstable atmosphere with large CAPE due to the strong low-level thermal forcing, which was very important in the energy supply for its development (Guofu and Shoujun, 2003; Zhu and Chen, 2003). Hence, the surface sensible heat flux and moving low-level vortex triggered by surface heating are considered two key factors to form a vertically unstable atmosphere that could induce MCSs.

Local circulations induced by the temperature differences from the land-surface heating are also important for the diurnal cycles of convective activities, especially in the southeastern and southern TP (Ye and Wu, 1998; Kurosaki and Kimura, 2002; Shu et al., 2013). One type of local circulation system that is induced by heterogeneous surface diabatic heating is the mountain-plains solenoid (MPS). MPSs can play an important role in the diurnal cycle of precipitation, e.g., by enhancing nocturnal precipitation of downstream mesoscale systems (e.g., in the leeward side of the eastern TP; Sun and Zhang, 2012; Bao and Zhang, 2013). Similar effects from MPSs have also been studied in other mountain regions, such as the Rockies (Carbone and Tuttle, 2008).

3.2.3 Orographic effects

What distinguishes convective precipitation over the TP from convection over land in the downstream regions is the interaction between convective systems and the complex topography. This interaction is also known as *orographic effect* which affects the amount, type, and duration of precipitation. The orographic effect contains three elements: moist and large-scale flow, orographic lifting, and condensation to precipitation (Rotunno and Houze, 2007). The effect is especially important to the deep convective cores that could develop into MCS at a later time by orographically lifting low-level warm and moist air, breaking a capping stable layer and leading to a more intensive convective system as well as broadening the stratiform region. Around the TP, convective activities and MCSs often occur on the south slope of the Himalayas due to low-level warm and moist air being transported into this region with dry air descending above from the mountains (Houze Jr et al., 2007; Romatschke et al., 2010; Kotal et al., 2014). Such examples can be also found in many high mountain areas such as the Andes

(e.g., Zuluaga and Houze, 2015; Warner et al., 2003), the Rocky Mountains (e.g., Houze Jr, 2012) and the Alpine (e.g., Morel and Senesi, 2002).

3.2.4 The role of microphysical processes

Microphysics processes are involved in the water phase changes between water vapor, cloud water, cloud ice, and precipitation. With intensive vertical motions within an MCS, the microphysics processes are essential for cloud structures as well as the amounts and locations of precipitation (Bryan and Morrison, 2012). A case of heavy precipitation originating from the TP was found to be enhanced with dominant rimming and aggregation processes due to the "seeder-feeder" mechanism, where the seeder was the original cloud system and the feeder was from low-level water vapor transportation (Chen Y. et al., 2020). The mechanism in this case though is not a typical "seeder-feeder" mechanism where the seeder clouds are widespread clouds and the low-level feeder clouds are forced by hills (Feng and Wang, 2011; Kim et al., 2022). Nevertheless, the microphysics processes are indeed essential to the MCSs development in this area. In numerical weather models, summer precipitation over the TP has been shown more sensitive to the cloud microphysics schemes than other parameterization schemes, such as planetary boundary layer and radiation schemes (Orr et al., 2017; Lv et al., 2020). Prein et al. (2022) also showed that the uncertainties of microphysics schemes are larger for cases of summer precipitation including an MCS case over the TP than that in winter, which points to the importance of further exploring the microphysics processes within MCSs.

3.3 Surface features

3.3.1 Snow cover and surface types

The heterogeneous land surface of the TP influences surface-atmosphere interactions such as momentum, heat, and water fluxes. Therefore, surface features can not be neglected when investigating the underlying mechanisms of the mesoscale organization of convection. For example, snow cover has been identified as a factor with indirect effects on convection and storm propagation through altering synoptic circulation patterns *via* heat flux changes (Lau and Kim, 2018; Luo and Lau, 2018). Luo and Lau (2018) and Lau and Kim (2018) found a statistical correlation between reduced snow cover and a strengthening of the South Asian High (SAH), which controls, for instance, storm tracks, MCSs (Kukulies et al., 2021) as well as precipitation features of TPVs (Feng et al., 2017). However, the direct influence of snow cover on the organization of mesoscale convection is not clear. Moreover, there are also possible interactions between glaciers and MCSs, which have not been explicitly addressed in the literature yet. Lin et al. (2021) suggested that Himalayan glaciers can retard the northward water vapor transport associated with the Asian summer monsoons and alter the local precipitation pattern. In consequence, the TP may become less moist, thereby unfavorable for the formation and development of MCSs. However, the proposed glacial effect on MCSs remains to be confirmed and high-resolution monitoring networks and/or modeling experiments might help investigate the latter.

3.3.2 Soil moisture and evapotranspiration

While Sugimoto and Ueno (2010) found a northwest-to-southeast soil moisture gradient and attributed this to the formation of MCSs in the southeastern parts of TP, new observations from the Global Change Observation Mission - Water (https://earth.jaxa.jp/en/data/products/soil-moisture/index.html) show a slightly different soil moisture distribution with the wettest areas in the central TP. Barton et al. (2021) also demonstrated that higher soil moisture content favors strong convection over the TP, but they also highlight this relationship was less evident when in regions with vegetation, more complex topography, or strong background winds. In addition; Hu et al. (2021) found that mesoscale soil moisture heterogeneity produced by early warm-season MCS rainfall promotes summer afternoon non-MCS rainfall, and soil moisture sourced from early MCS rainfall contribute to summer MCS rainfall because higher intensity MCS rainfall percolates into deeper soil that has a longer memory (Hu et al., 2020). Hence, these results call for a reconsideration of soil moisture as a major driver for convection, and other factors that can locally enhance moisture need to be contemplated.

The drier conditions in the northwest, which is also the main region for TPV genesis (Curio et al., 2018), could, on the other hand, explain the occurrence of dry vortex systems (Feng et al., 2014) in contrast to precipitating convective systems in the east (Hu et al., 2016). Since the genesis of TPV can partly be explained by the strong heating over dry land surfaces (Sugimoto and Ueno, 2010), surface conditions might affect the nature of storm systems over the TP and could be one of the determining factors which distinguishes TPVs from MCSs and smaller-scale convective cloud systems. Yamada and Uyeda (2006) and (Yamada, 2008) showed that the moisture supply through land and vegetation cover affects storm formation and precipitation intensity over the TP in a wet *versus* dry surface model experiment. However, it needs to be clarified to what extent vegetation and soil moisture can affect the convective precipitation component by altering surface energy balance and temperature. Pang et al. (2022) suggested that vegetation changes could dominate the variations of albedo that are closely related to the surface energy budget on the eastern and southern TP. In contrast, how exactly vegetation governs the surface heat fluxes and thereby controls MCS characteristics, is not known and the importance of moisture supply from land surfaces vs atmospheric large-scale transport for MCS genesis needs to be quantified.

3.3.3 Lake effect

While it is obvious that convection over the TP occurs mainly during the summer months when the monsoon circulation advects moisture to the inland and mountains, it has been suggested that vigorous convection can also result from the lake-effect snow, in regions of the plateau where large lakes are present. While lake-effect snow events are mesoscale systems with different dynamics from MCSs, they are also linked to convective instability and structures, as demonstrated by mesoscale numerical weather model simulations in the Great Lake region (e.g., Niziol et al., 1995; Kristovich et al., 2003). The relationship between the lake effect snow and convection over the TP has not been addressed in previous studies, but case studies of the lake effect in the TP have shown that it can be a frequent phenomenon that explains most of the winter variability in precipitation (Li et al., 2009; Kropacek et al., 2010; Dai et al., 2018).

The lake effect over large areas such as the Namco is also seen as a mesoscale moisture provider (Dai et al., 2020) and could hence contribute to storm formation during winter.

4 Challenges and opportunities

4.1 High-resolution regional climate modeling

The main challenge in simulating MCSs in regions with complex terrain is that state-of-the-art global reanalyses and conventional global and regional climate models have a relatively coarse spatial resolution (≥10 km), which is not sufficient to explicitly resolve deep convective processes and small-scale land-atmosphere interactions. Convection-permitting climate models provide a solution to this shortcoming because these are run with km-scale horizontal grid spacing, meaning that they do not have to rely on cumulus parameterization schemes.

Cumulus parameterization schemes have been widely regarded as one of the dominant sources of biases in modeling convection and precipitation, in particular in regions where multi-scale processes interact. For instance, the diurnal variations of precipitation over the TP, which is closely related to convective processes over complex terrain, exhibit large uncertainties associated with different cumulus parameterizations (Huang and Gao, 2017; Ou et al., 2020; Wang et al., 2021b). Simulating precipitation over the TP is therefore a long-standing challenge and most conventional climate models have a notable wet bias in this region. The improvements in simulating precipitation over the TP between the global model ensembles Coupled Model Intercomparison Project (CMIP) phase 3 (CMIP; Xu et al., 2010) (CMIP5; Su et al., 2013), and (CMIP6; Zhao et al., 2022) are almost negligible. This suggests that the cumulus parameterization and the coarse grid spacing in these global simulations are the main sources of uncertainty and that higher-resolution simulations are key to improving precipitation simulations.

Sato et al. (2008) attributed the wet bias over the TP to delayed cloud formation and too strong downward radiative fluxes that induces larger instability, thus resulting in an overestimation of heavy rainfall. Lin et al. (2018) showed that the wet bias could be reduced in simulations with really high resolution (i.e., 2 km) because the excessive water vapor transport into the TP is hampered by a more realistic orographic drag through a better-resolved topography of the central Himalayas. A similar reduction of the wet bias was also found by Li et al. (2021) who demonstrated that convection-permitting configurations of the Met Office Unified Model (MetUM) better captured the diurnal variations in precipitation as well as precipitation frequency, intensity, and structure over the TP. However, it still remains to be quantified whether the detected improvements can really be attributed to a better representation of MCSs and other elements of deep convection or if the improvements have other causes.

Once the reliability of convection-permitting climate simulations over the TP has been properly verified, they will help to significantly improve the understanding of the convective organization and other fundamental processes in the regional water cycle of the TP. In addition, they provide a new tool for application-based science because the reliable future projections of MCS-associated precipitation and its hydrological implications require that regional climate features are represented realistically. The current literature lacks studies with a focus on the link between MCS-associated precipitation, water availability for agriculture and flooding in the river basins around the TP, even though there exist several refined multi-decadal simulations that might be useful for this purpose (**Table 4**). These include, for instance, the High Asia Refined analysis (HAR; Maussion et al., 2014; Wang et al., 2021c) with a horizontal grid spacing of 10 km and a WRF-based downscaling product with a horizontal grid spacing of 9 km (Ou et al., 2020; 2023; **Table 4**). In addition, a CORDEX Flagship Pilot study named "Convection-Permitting Third Pole" (Prein et al., 2022) has been launched and endorsed by WCRP-CORDEX to coordinate the high-resolution modeling work focusing on MCSs and precipitation over the TP and its downstream regions. One goal of this project is to systematically investigate the sensitivities related to different modeling systems, model dynamics, and model physics, in order to define an optimal model configuration for multi-decadal past and future simulations over the TP. Most of the simulations in this project are run at grid spacing around 4 km and without cumulus parameterization, which offers new opportunities to improve our current understanding of the water cycle over and around the TP.

Another question that has not yet been solved for the TP region is the sensitivity of MCS simulations to the horizontal grid spacing. For example, Na et al. (2022) evaluated MCSs over China and the central United States based on a global non-hydrostatic model with 14 km grid spacing and found that warm-season MCSs were significantly underestimated in both regions. Some of the data sets in **Table 4** at gray-zone resolutions of around 10 km use a cumulus parameterization while others at similar grid spacings do not. An intercomparison of these data sets with regard to their ability to represent organized convection could help address this question, in order to define a reasonable minimum grid spacing to resolve a large portion of MCSs. Over the TP, the grid spacing might even need to be smaller than in flat regions due to its heterogeneous surface properties that can affect MCS formation (see **Section 3.3**). However, if the majority of convective systems over the TP occurs as single convective cells rather than larger-size MCSs (see **Section 2**), this could mean that a critical part of convective modes is still under-resolved in current convection-permitting simulations since a km-scale grid spacing is insufficient to resolve narrow updrafts and aspects of small-scale convection.

In particular, small-scale processes that influence the initiation and organization of convection such as entrainment and vertical mass fluxes are still parametrized (e.g., microphysical and planetary boundary layer parameterizations, land-atmosphere interactions). Because parameterization schemes often require tuning to specific cases and regions, the choice of parameterization scheme affects the representation of convective processes and results in different precipitation characteristics (Lv et al., 2020; Prein et al., 2022). In addition to that, the representation of convective processes is also influenced by the dynamic core of the model system and the general model configuration. For example, a case study within the CPTP project demonstrated that the performance in simulating a specific flood-producing MCS case in the Sichuan basin was strongly dependent on the underlying model, on the domain size,

TABLE 4 Overview of historical high-resolution regional climate model data sets covering the TP region.

Name	Reference and data availability	Regional model	Horizontal grid spacing	Temporal coverage	Spatial coverage	Cumulus parameterization?	Spectral nudging?
TP Reanalysis	Ou et al. (2020), Ou et al. (2023)[a]	ERA5-driven WRF	9 km	1979–2019	8 °N-50 °N, 65 °E-125 °E	None	Yes
High Asia Reanalysis (HARv1)	Maussion et al. (2014)[b]	FNL-driven WRF 3.3.1	30 km	2000–2014	0 °N-50 °N, 65 °E-110 °E	Grell 3D	No*
HARv1 (high-resolution)	Maussion et al. (2014)[b]	FNL-driven WRF 3.3.1	10 km	2000–2014	25 °N-40 °N, 72 °E-98 °E	Grell 3D	No*
HARv2	Wang et al. (2011)[c]	ERA5-driven WRF 4.1	10 km	1980–2020	20 °N-38 °N, 70 °E-105 °E	Grell 3D	No*
China Regional Reanalysis (CNRR)	Zhang et al. (2017)[d]	WRF	12 km	1976–2016	5 °N-60 °N, 30 °E-115 °E	Kain Fritsch	Yes
–	Gu et al. (2020)	ERA5-driven RegCM	10 km	1989–2008	20 °N-42 °N, 70 °E-105 °E	Kuo, Grell Emanuel, Kain, and Tiedtke	Yes
–	Bai et al. (2016)[e]	NCEP/DOEreanalysis-driven WRF	12 km	1979–2013	15 °N-65 °N 69 °E-140 °E	Kain Fritsch	No
–	Zhou et al. (2022)	ERA5-driven WRF 4.1	9 km	1999–2019	15 °N-45 °N, 68 °E-110 °E	None	Yes
–	Ma et al. (2022)	ERA5-driven WRF	3 km, 4 km, 9 km	2009–2018	20 °N-42 °N, 70 °E-110 °E	None	Yes
–	Pang et al. (2022)[f]	NCEP FNL Operational Model Global Tropospheric Analyses driven WRF3.1	10 km	2000–2010	25 °N-40 °N, 75 °E-105 °E	Kain Fritsch	No

* These datasets use daily reinitialization instead of spectral nudging to minimize the model drift.

[a] available at: http://biggeo.gvc.gu.se/TPReanalysis/

[b] available at: https://www.klima.tu-berlin.de/index.php?show=daten_har

[c] available at: https://www.klima.tu-berlin.de/index.php?show=daten_har2

[d] test simulation available at: https://share.weiyun.com/147d616b1cd8079756f1d728b9f41495, multi-year model data upon request.

[e] available at: https://data.tpdc.ac.cn/zh-hans/data/40895e03-f919-4721-893f-a6fee9feab81/

[f] available at: https://data.tpdc.ac.cn/zh-hans/data/58f4b08b-e88e-4652-b646-9e475039aa71

10.3389/feart.2023.1143380

and on the degree of large-scale constraint (i.e., if spectral nudging was used or not). These results suggest that a number of different choices may influence the representation of organized convection in regional climate simulations at km-scales. More research is needed to evaluate the representation of MCSs in these simulations from multiple perspectives so that reliable future predictions can be created over the TP. High-resolution and in particular convection-permitting simulations (≤4 km) have the potential to provide new insights into how MCSs, their impact on regional precipitation, and other related processes in the water cycle will change in a warmer climate. Due to the few existing convection-permitting simulations that extend into future periods, there are not many studies that have focused on future changes in MCS frequency and intensity in the downstream regions of the TP. This gap may be addressed with the help of newly emerging data sets which allow for MCS studies under different future scenarios.

Furthermore, data assimilation techniques can complement dynamical downscaling to create more robust historical climate data sets by combining model output with observations. Such techniques have been widely used in operating forecast systems, e.g., ECMWF-IFS (Europe), NCEP GFS (United States), and CMA-GFS (China). For example, Zhang et al. (2017) generated the China Regional Reanalysis (CNRR) with data assimilation and spectral nudging to improve the regional climate information over East Asia compared to ERA-Interim. In addition, a regional reanalysis of the TP has been produced with an ensemble Kalman filter (EnKF) data assimilation system and the experiments showed improvements in specific humidity, precipitation, and diurnal variation of precipitation over the TP (He et al., 2020).

4.2 Ground-based and space-borne observations

Observing snow and rain in remote mountain regions is a long-standing challenge (Li et al., 2022) which is why precipitation remains a major uncertainty in the water cycle over mountains. In particular, frozen precipitation is a major unknown in the mountain regions, and over the TP, it is likely that a large fraction of precipitation over the high altitudes occurs in the form of snow due to the low temperatures. In fact, Lundquist et al. (2019) pointed out that annual precipitation simulated by high-resolution atmospheric models over some mid-latitudinal mountain regions shows a better resemblance with ground-based streamflow and snowpack measurements than annual precipitation estimated from gridded data sets based on interpolated gauge measurements. This shows clearly that current observational datasets in these regions contain many uncertainties, but at the same time, we highly depend on these observations to have a reference against which models can be evaluated.

Prein et al. (2022) showed that discrepancies among different gridded observational data sets were the major source of uncertainty in an ensemble-based evaluation of case simulations over the TP. Hence, there is a need for high-density ground-based observations of snow and rain to be able to address outstanding challenges and model biases in convection-permitting climate modeling with respect to convection and precipitation in mountain regions. However, gauge measurements are still relatively sparse over the TP compared to those over eastern China, particularly over the upwind slope of the Himalayas and the higher elevated northwestern TP. Because most ground-based stations are located at lower elevations, gauge measurements capture the evening to nighttime precipitation peak associated with local-scale mountain-valley circulations (Chen et al., 2012; Lin et al., 2018; Ou et al., 2020). However, many stations do not represent the afternoon to late-afternoon rainfall peak associated with locations higher up on the mountain slopes (Chen et al., 2012; Ou et al., 2020). Therefore, high-density ground-based measurements with solid quality should be further constructed, developed, and regularly-maintained over the TP. While satellite retrievals of precipitation provide large coverage over remote regions, these measurements are more indirect than gauge measurements because they depend on the modeling of radiative transfer or machine learning. Gauge measurements are thus not only important as a direct reference for model evaluations, but also as a ground truth to improve satellite retrieval techniques and thereby create new useful observational data sets.

Advances in remote sensing of clouds and precipitation over the past 2 decades offer new possibilities to gain insights into cloud processes, and the full potential of satellite observations has likely not been used yet. For example, the vertical structure of MCSs in the TP region has not been extensively addressed. A better leverage of satellite observations beyond the commonly used gridded data products could help to more systematically evaluate the ability of high-resolution/convection-permitting simulations to represent MCSs and factors of organized convection that influence precipitation. Spaceborne cloud and precipitation radars provide the opportunity to view and assess simulated MCS characteristics by considering the vertical structure (e.g., Zhang et al., 2022). Because such active sensors are onboard polar-orbiting satellites, they provide only a limited spatial and temporal view through each scan. Therefore, they are not suitable to capture the full MCS life cycle and the vertical structure of MCSs can only be captured in snapshots rather than in a continuous way. They could, however, be used to evaluate long-term model data sets (see **Table 4**) that contain a lot of MCS samples so that climatological MCS characteristics can be inferred in a process-oriented manner. Combining the 3D structure of convection observed by spaceborne radars with MCS tracking from geostationary satellites (e.g., Futyan and Del Genio, 2007; Liu N. et al., 2021) provides additional insights into the evolution of MCS structures that could be used to evaluate convective-permitting model simulations. Additional satellite observations of cloud-related properties and other variables that are linked MCSs could be useful to address remaining uncertainties (e.g., uncertainties from the microphysical parameterization) in high-resolution simulations as they are more directly linked to convective processes than surface precipitation which may still be affected by parameter tuning.

A major drawback with satellite-derived surface precipitation is that it tends to significantly underestimate high rain rates from convective systems. For example, Cui et al. (2020a) found that occurrences of rain rates >10 mm h^{-1} in MCSs over the United States were significantly underestimated by IMERG compared to ground-based radars. This is due to sensor-related uncertainties and because gridded products like GPM IMERG represent average precipitation over a larger area rather than on a specific location. In addition, precipitation retrievals from passive microwave measurements over the TP contain large uncertainties because microwave

TABLE 5 Identified knowledge gaps and suggestions on how to address these.

	Identified knowledge gaps	Suggestions
Dynamic and thermodynamic processes	What are the different spatial scales of convective modes over the TP?	Quantify the occurrence of convection with different horizontal dimensions over the TP based on satellite observations and data assimilation products
	What is the role of capping inversions for lee cyclogenesis close to the TP?	Focus on factors that have been found relevant in other mountain regions in existing observational and model datasets (e.g., capping inversions)
	Remote vs local moisture sources - where does the moisture for MCSs come from?	Apply moisture tracking methods based on MCSs to establish a better understanding of where the moisture comes from
	The impact of seasonal to sub-seasonal variations in moisture transport on MCS variability	
	How do TPVs and MCSs interact on climatological time scales?	Perform object-based analyses (e.g., based on open-source libraries) of MCSs and other weather systems in historical convection-permitting climate simulations to study their interactions
	Feedbacks of MCSs to large-scale heat, moisture, and momentum redistribution	
	Land-atmosphere interactions (in particular the effect of snow and glacier surfaces on the convective organization)	
Modeling MCSs	Can the improvements in simulating precipitation characteristics over and around the TP with convection-permitting models be attributed to the better representation of MCSs?	Strengthen collaborations between the observation and modeling communities to better leverage ground-based and space-borne observations for the validation of convection-permitting model simulations and use data beyond the commonly gridded satellite products (e.g., include vertical structure) Assess the effect of biases in the large-scale circulation in model simulations on MCS genesis
	MCS populations in the TP region under different future scenarios	Coordinate modeling efforts between different communities to systematically assess uncertainties to ensure robust future simulations (see CORDEX Flagship Pilot Study CPTP)
Application-based science	Basin-scale quantification of MCS impact on seasonal streamflow and flood events	Study hydrological responses of MCSs in current historical and future simulations and observations, e.g., by using hydrological models or "ingredient-based approaches" Dougherty and Rasmussen, (2020) Strengthen collaboration with hydrologists
	MCS populations in the TP region under different future scenarios	Assess not only a potential increase in flooding, but also the possibility of droughts and water scarcity due to the absence of MCSs

retrievals are most challenging over snowy and icy surface types (Huffman et al., 2015; Dai et al., 2017). While these uncertainties may not significantly affect the detection rates of MCSs when using automated tracking methods, they hamper the evaluation of extreme storm cases and the quantification of the total amount of precipitation produced by an MCS. In addition, there are large discrepancies between different satellite-derived precipitation estimates over the TP, which make it currently difficult to use these data products to robustly validate high-resolution climate simulations (Ou et al., 2020). showed, for instance, that CMORPH microwave precipitation estimates exhibit notably larger mean precipitation amounts over lake regions than those from GPM IMERG.

Ground-based cloud and precipitation radars provide continuous observations of the vertical structure of MCSs through their entire lifetime (if the MCS is located within the radar scope). Such measurements might serve as a complement to spaceborne radars but are featured with a spatially limited coverage. While three-dimensional S-band radar mosaics that detect rainfall have been used to evaluate satellite-derived MCS characteristics over China in a few studies (Chen D. et al., 2020; Feng et al., 2021a), this data is generally difficult to access and limited to the downstream regions. Cloud radars over the TP such as from the measurements presented in (Uyeda et al., 2001) are mainly carried out during field experiments, thus providing insights on specific cases rather than climatological observations (Uyeda et al., 2001).

4.3 Object-based analyses of MCSs

The summarized results from various studies demonstrate that object-based analyses are indispensable for a process-oriented evaluation of organized convection in high-resolution satellite and model data sets. However, as shown in the previous sections, the choice of tracking criteria that are used for MCS identification considerably influences various MCS statistics

in a certain subregion. While these discrepancies might not be problematic when the same criteria are consistently used to compare the representation of MCSs in different datasets (e.g., observations vs models), they affect conclusions about the impact of MCSs on regional precipitation. In regions like the TP, it needs to be considered that the background climate is significantly different from other mid-latitude regions. In particular, there has been an overemphasis on MCSs over the high plateau when one single parameter is used to identify MCSs (i.e., brightness temperatures). The combination of different data sets and co-locations of various observations may help to address uncertainties related to tracking criteria and applied thresholds.

Given that MCS tracking over targeted regions is relevant for a wide range of scientific questions (i.e., climate dynamics, future changes in precipitation, and hydrological applications), the development of open source libraries for automated tracking is essential to allow different research communities to share their tools and knowledge. In addition, such libraries provide transparency, reproducibility, and eventually integrated testing that may reduce errors in the tracking method used. This is particularly useful for region-specific climate assessments that are often carried out by many different research groups. Two examples of open source tools for automated tracking and object-based analyses are tobac (*Tracking and object-based analysis of clouds*; Heikenfeld et al., 2019,; Sokolowsky et al. (*manuscript in prep.*) and PyFLEXTRKR (Feng et al., 2022; *preprint available at* https://doi.org/10.5194/egusphere-2022-1136).

5 Synthesis of knowledge gaps and future outlook

In summary, we find that there remain significant knowledge gaps about MCSs in the TP region despite the relatively high number of recent studies focusing on specific aspects of MCSs over and around the TP. **Table 5** presents the major knowledge gaps with regard to the understanding of dynamic and thermodynamic processes that are relevant for MCS genesis, model development and evaluation as well as open questions that are relevant for practical applications. We give suggestions on how the identified knowledge gaps can be addressed in future research based on existing and upcoming high-resolution data sets that were discussed in the previous section.

Author contributions

JK and H-WL designed the structure of the paper, conducted the literature research and wrote the first manuscript draft. DC contributed through supervision and participated in all discussions of the paper as well as in the writing process. JK created the figures and tables and coordinated the collaboration. All authors contributed in discussions, text editing, and the reviewing of relevant literature. All authors approved the final version.

Funding

This work was supported by the Swedish National Space Agency (188/18), Research Council (2019-03954), Formas (2017-01408) and STINT (CH2020-8767). ZF is supported by the United States Department of Energy Office of Science Biological and Environmental Research (BER) as part of the Regional and Global Climate Modeling program and the Atmospheric System Research program. PL is supported by the National Natural Science Foundation of China (Grant No. 42005039).

Acknowledgments

This work is a contribution to CORDEX-FPS-CPTP 14 and the Swedish national strategic research area MERGE.

Conflict of interest

The authors declare that the research was conducted in the absence of any commercial or financial relationships that could be construed as a potential conflict of interest.

Publisher's note

References

Asai, T., Ke, S., and Kodama, Y.-M. (1998). Diurnal variability of cloudiness over East Asia and the Western Pacific ocean as revealed by gms during the warm season. *J. Meteorological Soc. Jpn. Ser. II* 76, 675–684. doi:10.2151/jmsj1965.76.5_675

Bai, L. (2016). *Temperature and precipitation dataset of wrf model in northwest china (1979-2013)* . doi:10.11888/Meteoro.tpdc.270570

Bao, X., and Zhang, F. (2013). Impacts of the mountain–plains solenoid and cold pool dynamics on the diurnal variation of warm-season precipitation over northern China. *Atmos. Chem. Phys.* 13, 6965–6982. doi:10.5194/acp-13-6965-2013

Barton, E., Taylor, C., Klein, C., Harris, P., and Meng, X. (2021). Observed soil moisture impact on strong convection over mountainous Tibetan plateau. *J. Hydrometeorol.* 22, 561–572. doi:10.1175/jhm-d-20-0129.1

Bryan, G. H., and Morrison, H. (2012). Sensitivity of a simulated squall line to horizontal resolution and parameterization of microphysics. *Mon. Weather Rev.* 140, 202–225. doi:10.1175/mwr-d-11-00046.1

Carbone, R., Tuttle, J., Ahijevych, D., and Trier, S. (2002). Inferences of predictability associated with warm season precipitation episodes. *J. Atmos. Sci.* 59, 2033–2056. doi:10.1175/1520-0469(2002)059<2033:iopaww>2.0.co;2

Carbone, R., and Tuttle, J. (2008). Rainfall occurrence in the us warm season: The diurnal cycle. *J. Clim.* 21, 4132–4146. doi:10.1175/2008jcli2275.1

Chen, D., Guo, J., Yao, D., Feng, Z., and Lin, Y. (2020a). Elucidating the life cycle of warm-season mesoscale convective systems in eastern China from the himawari-8 geostationary satellite. *Remote Sens.* 12, 2307. doi:10.3390/rs12142307

Chen, D., Guo, J., Yao, D., Lin, Y., Zhao, C., Min, M., et al. (2019). Mesoscale convective systems in the Asian monsoon region from advanced himawari imager: Algorithms and preliminary results. *J. Geophys. Res. Atmos.* 124, 2210–2234. doi:10.1029/2018jd029707

Chen, H., Yuan, W., Li, J., and Yu, R. (2012). A possible cause for different diurnal variations of warm season rainfall as shown in station observations and trmm 3b42 data over the southeastern Tibetan plateau. *Adv. Atmos. Sci.* 29, 193–200. doi:10.1007/s00376-011-0218-1

Chen, W., Yang, S., and Huang, R.-H. (2005). Relationship between stationary planetary wave activity and the east Asian winter monsoon. *J. Geophys. Res. Atmos.* 110. doi:10.1029/2004jd005669

Chen, Y., and Li, Y. (2021). Convective characteristics and formation conditions in an extreme rainstorm on the eastern edge of the Tibetan plateau. *Atmosphere* 12, 381. doi:10.3390/atmos12030381

Chen, Y., Zhang, A., Zhang, Y., Cui, C., Wan, R., Wang, B., et al. (2020b). A heavy precipitation event in the yangtze river basin led by an eastward moving Tibetan plateau cloud system in the summer of 2016. *J. Geophys. Res. Atmos.* 125, e2020JD032429. doi:10.1029/2020jd032429

Choudhury, H., Roy, P., Kalita, S., and Sharma, S. (2016). Spatio-temporal variability of the properties of mesoscale convective systems over a complex terrain as observed by trmm sensors. *Int. J. Climatol.* 36, 2615–2632. doi:10.1002/joc.4516

Cui, W., Dong, X., Xi, B., Feng, Z., and Fan, J. (2020a). Can the gpm imerg final product accurately represent mcss' precipitation characteristics over the central and eastern United States? *J. Hydrometeorol.* 21, 39–57. doi:10.1175/jhm-d-19-0123.1

Cui, W., Dong, X., Xi, B., and Liu, M. (2020b). Cloud and precipitation properties of mcss along the meiyu frontal zone in central and southern China and their associated large-scale environments. *J. Geophys. Res. Atmos.* 125, e2019JD031601. doi:10.1029/2019jd031601

Curio, J., Chen, Y., Schiemann, R., Turner, A. G., Wong, K. C., Hodges, K., et al. (2018). Comparison of a manual and an automated tracking method for Tibetan plateau vortices. *Adv. Atmos. Sci.* 35, 965–980. doi:10.1007/s00376-018-7278-4

Curio, J., and Scherer, D. (2016). Seasonality and spatial variability of dynamic precipitation controls on the Tibetan plateau. *Earth Syst. Dyn.* 7, 767–782. doi:10.5194/esd-7-767-2016

Curio, J., Schiemannm, R., Hodges, K. I., and Turner, A. G. (2019). Climatology of Tibetan plateau vortices in reanalysis data and a high-resolution global climate model. *J. Clim.* 32, 1933–1950. doi:10.1175/jcli-d-18-0021.1

Dai, L., Che, T., Ding, Y., and Hao, X. (2017). Evaluation of snow cover and snow depth on the qinghai–Tibetan plateau derived from passive microwave remote sensing. *Cryosphere* 11, 1933–1948. doi:10.5194/tc-11-1933-2017

Dai, Y., Chen, D., Yao, T., and Wang, L. (2020). Large lakes over the Tibetan Plateau may boost snow downwind: Implications for snow disaster. *Sci. Bull.* 65, 1713–1717. doi:10.1016/j.scib.2020.06.012

Dai, Y., Yao, T., Li, X., and Ping, F. (2018). The impact of lake effects on the temporal and spatial distribution of precipitation in the nam co basin, Tibetan plateau. *Quat. Int.* 475, 63–69. doi:10.1016/j.quaint.2016.01.075

Dougherty, E., and Rasmussen, K. L. (2020). Changes in future flash flood–producing storms in the United States. *J. Hydrometeorol.* 21, 2221–2236. doi:10.1175/jhm-d-20-0014.1

Ehlers, T. A., Chen, D., Appel, E., Bolch, T., Chen, F., Diekmann, B., et al. (2022). Past, present, and future geo-biosphere interactions on the Tibetan plateau and implications for permafrost. *Earth-Science Rev.* 234, 104197. doi:10.1016/j.earscirev.2022.104197

Esmaili, R. B., Tian, Y., Vila, D. A., and Kim, K.-M. (2016). A Lagrangian analysis of cold cloud clusters and their life cycles with satellite observations. *J. Geophys. Res. Atmos.* 121, 11723–11738. doi:10.1002/2016jd025653

Feng, Z., Hardin, J., Barnes, H. C., Li, J., Leung, L. R., Varble, A., et al. (2022). PyFLEXTRKR: a Flexible Feature Tracking Python Software for Convective Cloud Analysis. *EGUsphere*, 1–29

Feng, L., and Zhou, T. (2012). Water vapor transport for summer precipitation over the Tibetan plateau: Multidata set analysis. *J. Geophys. Res. Atmos.* 117. doi:10.1029/2011jd017012

Feng, X., Liu, C., Fan, G., and Zhang, J. (2017). Analysis of the structure of different Tibetan plateau vortex types. *J. Meteorological Res.* 31, 514–529. doi:10.1007/s13351-017-6123-5

Feng, X., Liu, C., Rasmussen, R., and Fan, G. (2014). A 10-yr climatology of Tibetan plateau vortices with ncep climate forecast system reanalysis. *J. Appl. Meteorology Climatol.* 53, 34–46. doi:10.1175/jamc-d-13-014.1

Feng, Y.-C., and Wang, T.-C. C. (2011). Precipitation characteristics of an autumn torrential rainfall event in northern taiwan as determined from dual-polarization radar data. *J. Meteorological Soc. Jpn. Ser. II* 89, 133–150. doi:10.2151/jmsj.2011-203

Feng, Z., Houze, R. A., Jr, Leung, L. R., Song, F., Hardin, J. C., Wang, J., et al. (2019). Spatiotemporal characteristics and large-scale environments of mesoscale convective systems east of the rocky mountains. *J. Clim.* 32, 7303–7328. doi:10.1175/jcli-d-19-0137.1

Feng, Z., Leung, L. R., Houze, R. A., Jr, Hagos, S., Hardin, J., Yang, Q., et al. (2018). Structure and evolution of mesoscale convective systems: Sensitivity to cloud microphysics in convection-permitting simulations over the United States. *J. Adv. Model. Earth Syst.* 10, 1470–1494. doi:10.1029/2018ms001305

Feng, Z., Leung, L. R., Liu, N., Wang, J., Houze, R. A., Jr, Li, J., et al. (2021a). A global high-resolution mesoscale convective system database using satellite-derived cloud tops, surface precipitation, and tracking. *J. Geophys. Res. Atmos.* 126, e2020JD034202. doi:10.1029/2020jd034202

Feng, Z., Song, F., Sakaguchi, K., and Leung, L. R. (2021b). Evaluation of mesoscale convective systems in climate simulations: Methodological development and results from mpas-cam over the United States. *J. Clim.* 34, 2611–2633. doi:10.1175/jcli-d-20-0136.1

Flohn, H. (1957). "Large-scale aspects of the Summer Monsoon" in south and East Asia. *J. Meteorological Soc. Jpn. Ser. II* 35, 180–186. doi:10.2151/jmsj1923.35a.0_180

Flohn, H., and Reiter, E. R. (1968). *Contributions to a meteorology of the Tibetan highlands*. Libraries: Ph.D. thesis, Colorado State University.

Fu, R., Hu, Y., Wright, J. S., Jiang, J. H., Dickinson, R. E., Chen, M., et al. (2006). Short circuit of water vapor and polluted air to the global stratosphere by convective transport over the Tibetan plateau. *Proc. Natl. Acad. Sci.* 103, 5664–5669. doi:10.1073/pnas.0601584103

Fu, S.-M., Mai, Z., Sun, J.-H., Li, W.-L., Ding, Y., and Wang, Y.-Q. (2019). Impacts of convective activity over the Tibetan plateau on plateau vortex, southwest vortex, and downstream precipitation. *J. Atmos. Sci.* 76, 3803–3830. doi:10.1175/jas-d-18-0331.1

Fu, S., Mai, Z., Sun, J., Li, W., Zhong, Q., Sun, J., et al. (2021). A semi-idealized modeling study on the long-lived eastward propagating mesoscale convective system over the Tibetan plateau. *Sci. China Earth Sci.* 64, 1996–2014. doi:10.1007/s11430-020-9772-1

Fujinami, H., Nomura, S., and Yasunari, T. (2005). Characteristics of diurnal variations in convection and precipitation over the southern Tibetan plateau during summer. *Sola* 1, 49–52. doi:10.2151/sola.2005-014

Futyan, J. M., and Del Genio, A. D. (2007). Deep convective system evolution over Africa and the tropical atlantic. *J. Clim.* 20, 5041–5060. doi:10.1175/jcli4297.1

Gu, H., Yu, Z., Peltier, W. R., and Wang, X. (2020). Sensitivity studies and comprehensive evaluation of regcm4. 6.1 high-resolution climate simulations over the Tibetan plateau. *Clim. Dyn.* 54, 3781–3801. doi:10.1007/s00382-020-05205-6

Guo, Y., Du, Y., Lu, R., Feng, X., Li, J., Zhang, Y., et al. (2022). The characteristics of mesoscale convective systems generated over the yunnan–guizhou plateau during the warm seasons. *Int. J. Climatol.* 42, 7321–7341. doi:10.1002/joc.7647

Guo, Z.-y., Dai, X.-y., Wu, J.-p., and Lin, H. (2006). Analysis of mesoscale convective systems over Tibetan plateau in summer. *Chin. Geogr. Sci.* 16, 116–121. doi:10.1007/s11769-006-0004-7

Guofu, Z., and Shoujun, C. (2003). Analysis and comparison of mesoscale convective systems over the qinghai-xizang (Tibetan) plateau. *Adv. Atmos. Sci.* 20, 311–322. doi:10.1007/bf02690789

Haberlie, A. M., and Ashley, W. S. (2019). A radar-based climatology of mesoscale convective systems in the United States. *J. Clim.* 32, 1591–1606. doi:10.1175/jcli-d-18-0559.1

He, J., Yue, X., Le, H., Ren, Z., and Wan, W. (2020). Evaluation on the quasi-realistic ionospheric prediction using an ensemble kalman filter data assimilation algorithm. *Space weather.* 18, e2019SW002410. doi:10.1029/2019sw002410

Heikenfeld, M., Marinescu, P. J., Christensen, M., Watson-Parris, D., Senf, F., van den Heever, S. C., et al. (2019). Tobac 1.2: towards a flexible framework for tracking and analysis of clouds in diverse datasets. *Geosci. Model Dev.* 12, 4551–4570. doi:10.5194/gmd-12-4551-2019

Hirose, M., and Nakamura, K. (2005). Spatial and diurnal variation of precipitation systems over Asia observed by the trmm precipitation radar. *J. Geophys. Res. Atmos.* 110, D05106. doi:10.1029/2004jd004815

Houze, R. A., Jr (2004). Mesoscale convective systems. *Rev. Geophys.* 42. doi:10.1029/2004rg000150

Houze, R. A., Jr (2012). Orographic effects on precipitating clouds. *Rev. Geophys.* 50. doi:10.1029/2011rg000365

Houze, R. A., Jr, Rasmussen, K. L., Zuluaga, M. D., and Brodzik, S. R. (2015). The variable nature of convection in the tropics and subtropics: A legacy of 16 years of the tropical rainfall measuring mission satellite. *Rev. Geophys.* 53, 994–1021. doi:10.1002/2015rg000488

Houze, R. A., Jr, Wilton, D. C., and Smull, B. F. (2007). Monsoon convection in the himalayan region as seen by the trmm precipitation radar. *Q. J. R. Meteorological Soc. A J. Atmos. Sci. Appl. meteorology Phys. Oceanogr.* 133, 1389–1411. doi:10.1002/qj.106

Hu, H., Leung, L. R., and Feng, Z. (2021). Early warm-season mesoscale convective systems dominate soil moisture–precipitation feedback for summer rainfall in central United States. *Proc. Natl. Acad. Sci.* 118, e2105260118. doi:10.1073/pnas.2105260118

Hu, H., Leung, L. R., and Feng, Z. (2020). Understanding the distinct impacts of mcs and non-mcs rainfall on the surface water balance in the central United States using a

numerical water-tagging technique. *J. Hydrometeorol.* 21, 2343–2357. doi:10.1175/jhm-d-20-0081.1

Hu, L., Deng, D., Gao, S., and Xu, X. (2016). The seasonal variation of Tibetan convective systems: Satellite observation. *J. Geophys. Res. Atmos.* 121, 5512–5525. doi:10.1002/2015jd024390

Hu, L., Deng, D., Xu, X., and Zhao, P. (2017). The regional differences of Tibetan convective systems in boreal summer. *J. Geophys. Res. Atmos.* 122, 7289–7299. doi:10.1002/2017jd026681

Huang, D., and Gao, S. (2017). Impact of different cumulus convective parameterization schemes on the simulation of precipitation over China. *Tellus A Dyn. Meteorology Oceanogr.* 69, 1406264. doi:10.1080/16000870.2017.1406264

Huffman, G. J., Bolvin, D. T., Braithwaite, D., Hsu, K., Joyce, R., Xie, P., et al. (2015). "Nasa global precipitation measurement (gpm) integrated multi-satellite retrievals for gpm (imerg)," Algorithm Theoretical Basis Document (ATBD) Version 4.

Huffman, G. J., Bolvin, D. T., Nelkin, E. J., Stocker, E. F., and Tan, J. (2019). *V06 imerg release notes*. Greenbelt, MD, USA: NASA/GSFC.

Joyce, R. J., Janowiak, J. E., Arkin, P. A., and Xie, P. (2004). Cmorph: A method that produces global precipitation estimates from passive microwave and infrared data at high spatial and temporal resolution. *J. Hydrometeorol.* 5, 487–503. doi:10.1175/1525-7541(2004)005<0487:camtpg>2.0.co;2

Jun, L., Bin, W., and Dong-Hai, W. (2012). The characteristics of mesoscale convective systems (mcss) over East Asia in warm seasons. *Atmos. Ocean. Sci. Lett.* 5, 102–107. doi:10.1080/16742834.2012.11446973

Kim, H.-J., Jung, W., Suh, S.-H., Lee, D.-I., and You, C.-H. (2022). The characteristics of raindrop size distribution at windward and leeward side over mountain area. *Remote Sens.* 14, 2419. doi:10.3390/rs14102419

Kotal, S., Roy, S. S., and Bhowmik, S. R. (2014). Catastrophic heavy rainfall episode over uttarakhand during 16–18 june 2013–observational aspects. *Curr. Sci.* 107, 234–245.

Kristovich, D. A., Laird, N. F., and Hjelmfelt, M. R. (2003). Convective evolution across lake Michigan during a widespread lake-effect snow event. *Mon. Weather Rev.* 131, 643–655. doi:10.1175/1520-0493(2003)131<0643:cealmd>2.0.co;2

Kropacek, J., Feng, C., Alle, M., Kang, S., and Hochschild, V. (2010). Temporal and spatial aspects of snow distribution in the nam co basin on the Tibetan plateau from modis data. *Remote Sens.* 2, 2700–2712. doi:10.3390/rs2122700

Kukulies, J., Chen, D., and Curio, J. (2021). The role of mesoscale convective systems in precipitation in the Tibetan plateau region. *J. Geophys. Res. Atmos.* 126, e2021JD035279. doi:10.1029/2021jd035279

Kukulies, J., Chen, D., and Wang, M. (2019). Temporal and spatial variations of convection and precipitation over the Tibetan plateau based on recent satellite observations. part i: Cloud climatology derived from cloudsat and calipso. *Int. J. Climatol.* 39, 5396–5412. doi:10.1002/joc.6162

Kumar, A., Houze, R. A., Rasmussen, K. L., and Peters-Lidard, C. (2014). Simulation of a flash flooding storm at the steep edge of the himalayas. *J. Hydrometeorol.* 15, 212–228. doi:10.1175/jhm-d-12-0155.1

Kurosaki, Y., and Kimura, F. (2002). Relationship between topography and daytime cloud activity around Tibetan plateau. *J. Meteorological Soc. Jpn. Ser. II* 80, 1339–1355. doi:10.2151/jmsj.80.1339

Kuwagata, T. (1997). An analysis of summer rain showers over central Japan and its relation with the thermally induced circulation. *J. Meteorological Soc. Jpn. Ser. II* 75, 513–527. doi:10.2151/jmsj1965.75.2_513

Lai, H.-W., Chen, H. W., Kukulies, J., Ou, T., and Chen, D. (2021). Regionalization of seasonal precipitation over the Tibetan plateau and associated large-scale atmospheric systems. *J. Clim.* 34, 2635–2651. doi:10.1175/jcli-d-20-0521.1

Laing, A. G., and Michael Fritsch, J. (1997). The global population of mesoscale convective complexes. *Q. J. R. Meteorological Soc.* 123, 389–405. doi:10.1002/qj.49712353807

Lau, W. K., and Kim, K.-M. (2018). Impact of snow darkening by deposition of light-absorbing aerosols on snow cover in the himalayas–Tibetan Plateau and influence on the Asian summer monsoon: A possible mechanism for the blanford hypothesis. *Atmosphere* 9, 438. doi:10.3390/atmos9110438

Li, D., Qi, Y., and Chen, D. (2022). Changes in rain and snow over the Tibetan plateau based on imerg and ground-based observation. *J. Hydrology* 606, 127400. doi:10.1016/j.jhydrol.2021.127400

Li, M., Ma, Y., Hu, Z., Ishikawa, H., and Oku, Y. (2009). Snow distribution over the namco lake area of the Tibetan plateau. *Hydrology Earth Syst. Sci.* 13, 2023–2030. doi:10.5194/hess-13-2023-2009

Li, P., Furtado, K., Zhou, T., Chen, H., and Li, J. (2021). Convection-permitting modelling improves simulated precipitation over the central and eastern Tibetan plateau. *Q. J. R. Meteorological Soc.* 147, 341–362. doi:10.1002/qj.3921

Li, P., Guo, Z., Furtado, K., Chen, H., Li, J., Milton, S., et al. (2019). Prediction of heavy precipitation in the eastern China flooding events of 2016: Added value of convection-permitting simulations. *Q. J. R. Meteorological Soc.* 145, 3300–3319. doi:10.1002/qj.3621

Li, P., Moseley, C., Prein, A. F., Chen, H., Li, J., Furtado, K., et al. (2020). Mesoscale convective system precipitation characteristics over East Asia. part i: Regional differences and seasonal variations. *J. Clim.* 33, 9271–9286. doi:10.1175/jcli-d-20-0072.1

Li, Y., and Zhang, M. (2017). The role of shallow convection over the Tibetan Plateau. *J. Clim.* 30 (15), 5791–5803

Lin, C., Chen, D., Yang, K., and Ou, T. (2018). Impact of model resolution on simulating the water vapor transport through the central himalayas: Implication for models' wet bias over the Tibetan Plateau. *Clim. Dyn.* 51, 3195–3207. doi:10.1007/s00382-018-4074-x

Lin, C., Yang, K., Chen, D., Guyennon, N., Balestrini, R., Yang, X., et al. (2021). Summer afternoon precipitation associated with wind convergence near the himalayan glacier fronts. *Atmos. Res.* 259, 105658. doi:10.1016/j.atmosres.2021.105658

Liu, B., Wu, G., Mao, J., and He, J. (2013). Genesis of the south Asian high and its impact on the Asian summer monsoon onset. *J. Clim.* 26, 2976–2991. doi:10.1175/jcli-d-12-00286.1

Liu, N., Leung, L. R., and Feng, Z. (2021a). Global mesoscale convective system latent heating characteristics from gpm retrievals and an mcs tracking dataset. *J. Clim.* 34, 8599–8613. doi:10.1175/jcli-d-20-0997.1

Liu, Y., Yao, X., Fei, J., Yang, X., and Sun, J. (2021b). Characteristics of mesoscale convective systems during the warm season over the Tibetan plateau based on fy-2 satellite datasets. *Int. J. Climatol.* 41, 2301–2315. doi:10.1002/joc.6959

Lundquist, J., Hughes, M., Gutmann, E., and Kapnick, S. (2019). Our skill in modeling mountain rain and snow is bypassing the skill of our observational networks. *Bull. Am. Meteorological Soc.* 100, 2473–2490. doi:10.1175/bams-d-19-0001.1

Luo, H., and Yanai, M. (1984). The large-scale circulation and heat sources over the Tibetan plateau and surrounding areas during the early summer of 1979. part ii: Heat and moisture budgets. *Mon. Weather Rev.* 112, 966–989. doi:10.1175/1520-0493(1984)112<0966:tlscah>2.0.co;2

Luo, M., and Lau, N.-C. (2018). Synoptic characteristics, atmospheric controls, and long-term changes of heat waves over the indochina peninsula. *Clim. Dyn.* 51, 2707–2723. doi:10.1007/s00382-017-4038-6

Lv, M., Xu, Z., and Yang, Z.-L. (2020). Cloud resolving wrf simulations of precipitation and soil moisture over the central Tibetan Plateau: An assessment of various physics options. *Earth Space Sci.* 7, e2019EA000865. doi:10.1029/2019ea000865

Ma, M., Hui, P., Liu, D., Zhou, P., and Tang, J. (2022). Convection-permitting regional climate simulations over Tibetan Plateau: Re-initialization versus spectral nudging. *Clim. Dyn.* 58, 1719–1735. doi:10.1007/s00382-021-05988-2

Maddox, R. A. (1980). Meoscale convective complexes. *Bull. Am. Meteorological Soc.* 61, 1374–1387. doi:10.1175/1520-0477(1980)061<1374:mcc>2.0.co;2

Mai, Z., Fu, S.-M., Sun, J.-H., Hu, L., and Wang, X.-m. (2021). Key statistical characteristics of the mesoscale convective systems generated over the Tibetan plateau and their relationship to precipitation and southwest vortices. *Int. J. Climatol.* 41, E875–E896. doi:10.1002/joc.6735

Maussion, F., Scherer, D., Mölg, T., Collier, E., Curio, J., and Finkelnburg, R. (2014). Precipitation seasonality and variability over the Tibetan plateau as resolved by the high Asia reanalysis. *J. Clim.* 27, 1910–1927. doi:10.1175/jcli-d-13-00282.1

Meng, Y., Sun, J., Zhang, Y., and Fu, S. (2021). A 10-year climatology of mesoscale convective systems and their synoptic circulations in the southwest mountain area of China. *J. Hydrometeorol.* 22, 23–41. doi:10.1175/jhm-d-20-0167.1

Morel, C., and Senesi, S. (2002). A climatology of mesoscale convective systems over Europe using satellite infrared imagery. ii: Characteristics of European mesoscale convective systems. *Q. J. R. Meteorological Soc. A J. Atmos. Sci. Appl. meteorology Phys. Oceanogr.* 128, 1973–1995. doi:10.1256/003590002320603494

Na, Y., Fu, Q., Leung, L. R., Kodama, C., and Lu, R. (2022). Mesoscale convective systems simulated by a high-resolution global nonhydrostatic model over the United States and China. *J. Geophys. Res. Atmos.* 127, e2021JD035916. doi:10.1029/2021jd035916

Niziol, T. A., Snyder, W. R., and Waldstreicher, J. S. (1995). Winter weather forecasting throughout the eastern United States. part iv: Lake effect snow. *Weather Forecast.* 10, 61–77. doi:10.1175/1520-0434(1995)010<0061:wwftte>2.0.co;2

Ohsawa, T., Ueda, H., Hayashi, T., Watanabe, A., and Matsumoto, J. (2001). Diurnal variations of convective activity and rainfall in tropical Asia. *J. Meteorological Soc. Jpn. Ser. II* 79, 333–352. doi:10.2151/jmsj.79.333

Orr, A., Listowski, C., Couttet, M., Collier, E., Immerzeel, W., Deb, P., et al. (2017). Sensitivity of simulated summer monsoonal precipitation in langtang valley, himalaya, to cloud microphysics schemes in wrf. *J. Geophys. Res. Atmos.* 122, 6298–6318. doi:10.1002/2016jd025801

Ou, T., Chen, D., Chen, X., Lin, C., Yang, K., Lai, H.-W., et al. (2020). Simulation of summer precipitation diurnal cycles over the Tibetan plateau at the gray-zone grid spacing for cumulus parameterization. *Clim. Dyn.* 54, 3525–3539. doi:10.1007/s00382-020-05181-x

Ou, T., Chen, D., Tang, J., Lin, C., Wang, X., Kukulies, J., et al. (2023). Wet bias of summer precipitation in the northwestern Tibetan plateau in era5 is linked to overestimated lower-level southerly wind over the plateau. *Clim. Dyn.*, 1–15. doi:10.1007/s00382-023-06672-3

Pang, G., Chen, D., Wang, X., and Lai, H.-W. (2022). Spatiotemporal variations of land surface albedo and associated influencing factors on the Tibetan plateau. *Sci. Total Environ.* 804, 150100. doi:10.1016/j.scitotenv.2021.150100

Pendergrass, A. G. (2020). Changing degree of convective organization as a mechanism for dynamic changes in extreme precipitation. *Curr. Clim. change Rep.* 6, 47–54. doi:10.1007/s40641-020-00157-9

Pendergrass, A. G., Reed, K. A., and Medeiros, B. (2016). The link between extreme precipitation and convective organization in a warming climate: Global radiative-convective equilibrium simulations. *Geophys. Res. Lett.* 43, 11–445. doi:10.1002/2016gl071285

Prein, A. F., Ban, N., Ou, T., Tang, J., Sakaguchi, K., Collier, E., et al. (2022). Towards ensemble-based kilometer-scale climate simulations over the third pole region. *Clim. Dyn.*, 1–27. doi:10.1007/s00382-022-06543-3

Prein, A. F., Liu, C., Ikeda, K., Bullock, R., Rasmussen, R. M., Holland, G. J., et al. (2020). Simulating north American mesoscale convective systems with a convection-permitting climate model. *Clim. Dyn.* 55, 95–110. doi:10.1007/s00382-017-3993-2

Prein, A. F., Liu, C., Ikeda, K., Trier, S. B., Rasmussen, R. M., Holland, G. J., et al. (2017). Increased rainfall volume from future convective storms in the us. *Nat. Clim. Change* 7, 880–884. doi:10.1038/s41558-017-0007-7

Qie, X., Wu, X., Yuan, T., Bian, J., and Lu, D. (2014). Comprehensive pattern of deep convective systems over the Tibetan plateau–south Asian monsoon region based on trmm data. *J. Clim.* 27, 6612–6626. doi:10.1175/jcli-d-14-00076.1

Rasmussen, K. L., and Houze, R. A. (2012). A flash-flooding storm at the steep edge of high terrain: Disaster in the himalayas. *Bull. Am. Meteorological Soc.* 93, 1713–1724. doi:10.1175/bams-d-11-00236.1

Roca, R., and Fiolleau, T. (2020). Extreme precipitation in the tropics is closely associated with long-lived convective systems. *Commun. Earth Environ.* 18 (1), 1–6. doi:10.1038/s43247-020-00015-4

Romatschke, U., and Houze, R. A. (2011). Characteristics of precipitating convective systems in the south Asian monsoon. *J. Hydrometeorol.* 12, 3–26. doi:10.1175/2010jhm1289.1

Romatschke, U., Medina, S., and Houze, R. A. (2010). Regional, seasonal, and diurnal variations of extreme convection in the south Asian region. *J. Clim.* 23, 419–439. doi:10.1175/2009jcli3140.1

Rossow, W. B., Mekonnen, A., Pearl, C., and Goncalves, W. (2013). Tropical precipitation extremes. *J. Clim.* 26, 1457–1466. doi:10.1175/jcli-d-11-00725.1

Rotunno, R., and Houze, R. A. (2007). Lessons on orographic precipitation from the mesoscale alpine programme. *Q. J. R. Meteorological Soc. A J. Atmos. Sci. Appl. meteorology Phys. Oceanogr.* 133, 811–830. doi:10.1002/qj.67

Sato, T., Yoshikane, T., Satoh, M., Miura, H., and Fujinami, H. (2008). Resolution dependency of the diurnal cycle of convective clouds over the Tibetan plateau in a mesoscale model. *J. Meteorological Soc. Jpn. Ser. II* 86, 17–31. doi:10.2151/jmsj.86a.17

Schiemann, R., Lüthi, D., and Schär, C. (2009). Seasonality and interannual variability of the westerly jet in the Tibetan plateau region. *J. Clim.* 22, 2940–2957. doi:10.1175/2008jcli2625.1

Schumacher, R. S., and Rasmussen, K. L. (2020). The formation, character and changing nature of mesoscale convective systems. *Nat. Rev. Earth Environ.* 1, 300–314. doi:10.1038/s43017-020-0057-7

Shu, Y., Pan, Y., and Wang, J. (2013). Diurnal variation of mcss over Asia and the Western Pacific region. *Acta Meteorol. Sin.* 27, 435–445. doi:10.1007/s13351-013-0305-6

Song, F., Feng, Z., Leung, L. R., Pokharel, B., Wang, S.-Y. S., Chen, X., et al. (2021). Crucial roles of eastward propagating environments in the summer mcs initiation over the us great plains. *J. Geophys. Res. Atmos.* 126, e2021JD034991. doi:10.1029/2021jd034991

Su, F., Duan, X., Chen, D., Hao, Z., and Cuo, L. (2013). Evaluation of the global climate models in the cmip5 over the Tibetan plateau. *J. Clim.* 26, 3187–3208. doi:10.1175/jcli-d-12-00321.1

Sugimoto, S. (2020). Heavy precipitation over southwestern Japan during the baiu season due to abundant moisture transport from synoptic-scale atmospheric conditions. *SOLA* 16, 17–22. doi:10.2151/sola.2020-004

Sugimoto, S., and Ueno, K. (2010). Formation of mesoscale convective systems over the eastern Tibetan plateau affected by plateau-scale heating contrasts. *J. Geophys. Res. Atmos.* 115, D16105. doi:10.1029/2009jd013609

Sugimoto, S., and Ueno, K. (2012). Role of mesoscale convective systems developed around the eastern Tibetan plateau in the eastward expansion of an upper tropospheric high during the monsoon season. *J. Meteorological Soc. Jpn. Ser. II* 90, 297–310. doi:10.2151/jmsj.2012-209

Sun, J., and Zhang, F. (2012). Impacts of mountain–plains solenoid on diurnal variations of rainfalls along the mei-yu front over the east China plains. *Mon. Weather Rev.* 140, 379–397. doi:10.1175/mwr-d-11-00041.1

Tao, S.-y., and Ding, Y.-h. (1981). Observational evidence of the influence of the qinghai-xizang (tibet) plateau on the occurrence of heavy rain and severe convective storms in China. *Bull. Am. Meteorological Soc.* 62, 23–30. doi:10.1175/1520-0477(1981)062<0023:oeotio>2.0.co;2

Tucker, D. F., and Crook, N. A. (1999). The generation of a mesoscale convective system from mountain convection. *Mon. weather Rev.* 127, 1259–1273. doi:10.1175/1520-0493(1999)127<1259:tgoamc>2.0.co;2

Uyeda, H., Yamada, H., Horikomi, J., Shirooka, R., Shimizu, S., Liping, L., et al. (2001). Characteristics of convective clouds observed by a Doppler radar at naqu on Tibetan plateau during the game-tibet iop. *J. Meteorological Soc. Jpn. Ser. II* 79, 463–474. doi:10.2151/jmsj.79.463

Ueno, K., Sugimoto, S., Koike, T., Tsutsui, H., and Xu, X. (2011). Generation processes of mesoscale convective systems following midlatitude troughs around the Sichuan Basin. *J. Geophys. Res. Atmos.* 116 (D2)

Virts, K. S., and Houze, R. A. (2016). Seasonal and intraseasonal variability of mesoscale convective systems over the south Asian monsoon region. *J. Atmos. Sci.* 73, 4753–4774. doi:10.1175/jas-d-16-0022.1

Wang, S.-Y., Chen, T.-C., and Takle, E. S. (2011). Climatology of summer midtropospheric perturbations in the us northern plains. part ii: Large-scale effects of the rocky mountains on Genesis. *Clim. Dyn.* 36, 1221–1237. doi:10.1007/s00382-010-0765-7

Wang, S., Yang, Y., Gong, W., Che, Y., Ma, X., and Xie, J. (2021a). Reason analysis of the jiwenco glacial lake outburst flood (glof) and potential hazard on the qinghai-Tibetan plateau. *Remote Sens.* 13, 3114. doi:10.3390/rs13163114

Wang, X., Chen, D., Pang, G., Anwar, S. A., Ou, T., and Yang, M. (2021b). Effects of cumulus parameterization and land-surface hydrology schemes on Tibetan Plateau climate simulation during the wet season: Insights from the regcm4 model. *Clim. Dyn.* 57, 1853–1879. doi:10.1007/s00382-021-05781-1

Wang, X., Tolksdorf, V., Otto, M., and Scherer, D. (2021c). Wrf-based dynamical downscaling of era5 reanalysis data for high mountain Asia: Towards a new version of the high Asia refined analysis. *Int. J. Climatol.* 41, 743–762. doi:10.1002/joc.6686

Warner, T. T., Mapes, B. E., and Xu, M. (2003). Diurnal patterns of rainfall in northwestern south America. part ii: Model simulations. *Mon. Weather Rev.* 131, 813–829. doi:10.1175/1520-0493(2003)131<0813:dporin>2.0.co;2

Xia, R., Luo, Y., Zhang, D.-L., Li, M., Bao, X., and Sun, J. (2021). On the diurnal cycle of heavy rainfall over the sichuan basin during 10–18 august 2020. *Adv. Atmos. Sci.* 38, 2183–2200. doi:10.1007/s00376-021-1118-7

Xu, W., and Zipser, E. J. (2011). Diurnal variations of precipitation, deep convection, and lightning over and east of the eastern Tibetan plateau. *J. Clim.* 24, 448–465. doi:10.1175/2010jcli3719.1

Xu, X., Shi, X., Wang, Y., Peng, S., and Shi, X. (2008). Data analysis and numerical simulation of moisture source and transport associated with summer precipitation in the yangtze river valley over China. *Meteorology Atmos. Phys.* 100, 217–231. doi:10.1007/s00703-008-0305-8

Xu, Y., Gao, X., and Giorgi, F. (2010). Upgrades to the reliability ensemble averaging method for producing probabilistic climate-change projections. *Clim. Res.* 41, 61–81. doi:10.3354/cr00835

Yamada, H. (2008). Numerical simulations of the role of land surface conditions in the evolution and structure of summertime thunderstorms over a flat highland. *Mon. weather Rev.* 136, 173–188. doi:10.1175/2007mwr2053.1

Yamada, H., and Uyeda, H. (2006). Transition of the rainfall characteristics related to the moistening of the land surface over the central Tibetan plateau during the summer of 1998. *Mon. weather Rev.* 134, 3230–3247. doi:10.1175/mwr3235.1

Yanai, M., and Li, C. (1994). Mechanism of heating and the boundary layer over the Tibetan plateau. *Mon. Weather Rev.* 122, 305–323. doi:10.1175/1520-0493(1994)122<0305:mohatb>2.0.co;2

Yanai, M., Li, C., and Song, Z. (1992). Seasonal heating of the Tibetan plateau and its effects on the evolution of the Asian summer monsoon. *J. Meteorological Soc. Jpn. Ser. II* 70, 319–351. doi:10.2151/jmsj1965.70.1b_319

Yang, K., Koike, T., Fujii, H., Tamura, T., Xu, X., Bian, L., et al. (2004). The daytime evolution of the atmospheric boundary layer and convection over the Tibetan Plateau: Observations and simulations. *J. Meteorological Soc. Jpn. Ser. II* 82, 1777–1792. doi:10.2151/jmsj.82.1777

Yang, M., Wang, X., Pang, G., Wan, G., and Liu, Z. (2019a). The Tibetan plateau cryosphere: Observations and model simulations for current status and recent changes. *Earth-Science Rev.* 190, 353–369. doi:10.1016/j.earscirev.2018.12.018

Yang, Q., Houze, R. A., Jr, Leung, L. R., and Feng, Z. (2017). Environments of long-lived mesoscale convective systems over the central United States in convection permitting climate simulations. *J. Geophys. Res. Atmos.* 122, 13–288. doi:10.1002/2017jd027033

Yang, R., Zhang, Y., Sun, J., Fu, S., and Li, J. (2019b). The characteristics and classification of eastward-propagating mesoscale convective systems generated over the second-step terrain in the yangtze river valley. *Atmos. Sci. Lett.* 20, e874. doi:10.1002/asl.874

Yang, X., Fei, J., Huang, X., Cheng, X., Carvalho, L. M., and He, H. (2015). Characteristics of mesoscale convective systems over China and its vicinity using geostationary satellite fy2. *J. Clim.* 28, 4890–4907. doi:10.1175/jcli-d-14-00491.1

Yao, T., Bolch, T., Chen, D., Gao, J., Immerzeel, W., Piao, S., et al. (2022). The imbalance of the Asian water tower. *Nat. Rev. Earth Environ.* 3, 618–632. –15. doi:10.1038/s43017-022-00299-4

Yaodong, L., Yun, W., Yang, S., Liang, H., Shouting, G., and Fu, R. (2008). Characteristics of summer convective systems initiated over the Tibetan plateau. part i: Origin, track, development, and precipitation. *J. Appl. Meteorology Climatol.* 47, 2679–2695. doi:10.1175/2008jamc1695.1

Yasunari, T., and Miwa, T. (2006). Convective cloud systems over the Tibetan Plateau and their impact on meso-scale disturbances in the meiyu/baiu frontal zone. *J. Meteorological Soc. Jpn. Ser. II* 84, 783–803. doi:10.2151/jmsj.84.783

Ye, D.-Z., and Wu, G.-X. (1998). The role of the heat source of the Tibetan plateau in the general circulation. *Meteorology Atmos. Phys.* 67, 181–198. doi:10.1007/bf01277509

Yeh, T.-C. (1957). The wind structure and heat balance in the lower troposphere over the Tibetan plateau and its surroundings. *Acta. Meteor. Sin.* 28, 108–121.

You, Q., Cai, Z., Pepin, N., Chen, D., Ahrens, B., Jiang, Z., et al. (2021). Warming amplification over the arctic pole and third pole: Trends, mechanisms and consequences. *Earth-Science Rev.* 217, 103625. doi:10.1016/j.earscirev.2021.103625

Yu, S. (2001). Primary study on the impact of Tibetan plateau weather systems on the big flood peaks of the yangtze river in 1998. *Mech. Predict. 1998 Extreme Rainfall over Yangtze River Basin Nenjiang Val.*, 359–364.

Yuan, J., and Houze, R. A. (2010). Global variability of mesoscale convective system anvil structure from a-train satellite data. *J. Clim.* 23, 5864–5888. doi:10.1175/2010jcli3671.1

Yun, Y., Liu, C., Luo, Y., and Gao, W. (2021). Warm-season mesoscale convective systems over eastern China: Convection-permitting climate model simulation and observation. *Clim. Dyn.* 57, 3599–3617. doi:10.1007/s00382-021-05994-4

Zhang, A., Chen, C., Chen, Y., Li, W., Chen, S., and Fu, Y. (2022). Resilient dataset of rain clusters with life cycle evolution during april to june 2016–2020 over eastern Asia based on observations from the gpm dpr and himawari-8 ahi. *Earth Syst. Sci. Data* 14, 1433–1445. doi:10.5194/essd-14-1433-2022

Zhang, L., Su, F., Yang, D., Hao, Z., and Tong, K. (2013). Discharge regime and simulation for the upstream of major rivers over Tibetan plateau. *J. Geophys. Res. Atmos.* 118, 8500–8518. doi:10.1002/jgrd.50665

Zhang, Q., Pan, Y., Wang, S., Xu, J., and Tang, J. (2017). High-resolution regional reanalysis in China: Evaluation of 1 year period experiments. *J. Geophys. Res. Atmos.* 122, 10,801–10,819. doi:10.1002/2017jd027476

Zhang, X., Shen, W., Zhuge, X., Yang, S., Chen, Y., Wang, Y., et al. (2021). Statistical characteristics of mesoscale convective systems initiated over the Tibetan plateau in summer by fengyun satellite and precipitation estimates. *Remote Sens.* 13, 1652. doi:10.3390/rs13091652

Zhao, Y., Zhou, T., Zhang, W., and Li, J. (2022). Change in precipitation over the Tibetan plateau projected by weighted cmip6 models. *Adv. Atmos. Sci.* 39, 1133–1150. doi:10.1007/s00376-022-1401-2

Zheng, Y., Chen, J., and Zhu, P. (2008). Climatological distribution and diurnal variation of mesoscale convective systems over China and its vicinity during summer. *Chin. Sci. Bull.* 53, 1574–1586. doi:10.1007/s11434-008-0116-9

Zhou, P., Shao, M., Ma, M., Ou, T., and Tang, J. (2022). Wrf gray-zone dynamical downscaling over the Tibetan Plateau during 1999–2019: Model performance and added value. *Clim. Dyn.*, 1–20. doi:10.1007/s00382-022-06631-4

Zhu, G., and Chen, S. (2003). A numerical case study on a mesoscale convective system over the qinghai-xizang (Tibetan) plateau. *Adv. Atmos. Sci.* 20, 385–397. doi:10.1007/bf02690797

Zipser, E. J., Cecil, D. J., Liu, C., Nesbitt, S. W., and Yorty, D. P. (2006). Where are the most intense thunderstorms on Earth? *Bull. Am. Meteorological Soc.* 87, 1057–1072. doi:10.1175/bams-87-8-1057

Zuluaga, M. D., and Houze, R. A. (2015). Extreme convection of the near-equatorial americas, Africa, and adjoining oceans as seen by trmm. *Mon. Weather Rev.* 143, 298–316. doi:10.1175/mwr-d-14-00109.1